SPECIAL Connecting the Tropics to the Polar Regions COLLECTION

REVIEW

The Interconnected Global Climate System—A Review of Tropical–Polar Teleconnections

XIAOJUN YUAN, MICHAEL R. KAPLAN, AND MARK A. CANE

Lamont-Doherty Earth Observatory, Columbia University, Palisades, New York

(Manuscript received 29 August 2016, in final form 13 December 2017)

ABSTRACT

This paper summarizes advances in research on tropical–polar teleconnections, made roughly over the last decade. Elucidating El Niño–Southern Oscillation (ENSO) impacts on high latitudes has remained an important focus along different lines of inquiry. Tropical to polar connections have also been discovered at the intraseasonal time scale, associated with Madden–Julian oscillations (MJOs). On the time scale of decades, changes in MJO phases can result in temperature and sea ice changes in the polar regions of both hemispheres. Moreover, the long-term changes in SST of the western tropical Pacific, tropical Atlantic, and North Atlantic Ocean have been linked to the rapid winter warming around the Antarctic Peninsula, while SST changes in the central tropical Pacific have been linked to the warming in West Antarctica. Rossby wave trains emanating from the tropics remain the key mechanism for tropical and polar teleconnections from intraseasonal to decadal time scales. ENSO-related tropical SST anomalies affect higher-latitude annular modes by modulating mean zonal winds in both the subtropics and midlatitudes. Recent studies have also revealed the details of the interactions between the Rossby wave and atmospheric circulations in high latitudes. We also review some of the hypothesized connections between the tropics and poles in the past, including times when the climate was fundamentally different from present day especially given a larger-than-present-day global cryosphere. In addition to atmospheric Rossby waves forced from the tropics, large polar temperature changes and amplification, in part associated with variability in orbital configuration and solar irradiance, affected the low–high-latitude connections.

1. Introduction

Improving our understanding of the dynamics of the atmosphere–ocean–sea ice system and the connecting mechanisms between the high and low latitudes has become increasingly important to climate science in the face of a rapidly warming world. The polar regions and the cryosphere in both hemispheres are active components in global climate. For example, changes within the polar regions dictate the strength of the thermal gradient between the tropics and the poles.

Climate changes have been observed in both of Earth's polar regions over the past several decades and have been magnified in the last ~10 years in terms of recorded sea ice extent (SIE) and surface temperatures. For example, in September 2012 Arctic sea ice extent set a new record low in more than three decades of satellite observations, while Antarctic sea ice extent reached a record high for the same period, reported by the National Snow and Ice Data Center (http://nsidc.org/cryosphere/sotc/sea_ice.html). While September Arctic SIE has slightly recovered since 2013, Antarctic SIE continued to reach record highs until 2014, followed by a drop in 2016 and 2017.

Near-surface temperatures in the Arctic region show a warming of ~0.7 K decade^{-1} (Cavalieri and Parkinson 2012), which reflects primarily an ice-albedo feedback. Since Antarctic sea ice mostly melts back to the coast in summer when the sun returns to the Southern Hemisphere (SH) and albedo is highly correlated with sea ice concentration (SIC; Shao and Ke 2015), the ice-albedo feedback is not as important as it is in northern high latitudes. There is no consistent sea surface temperature (SST) warming. Instead, surface temperatures show a strong spatial contrast, with rapid warming (~0.35°C decade^{-1}) around the Antarctic Peninsula (AP) and a net cooling in East Antarctica (Chapman and Walsh 2007; O'Donnell et al. 2011; Turner 2016).

Corresponding author: Xiaojun Yuan, xyuan@ldeo.columbia.edu

DOI: 10.1175/JCLI-D-16-0637.1

Studies had attributed the Antarctic cooling and sea ice expansion to ozone depletion (Thompson and Solomon 2002; Turner et al. 2009). However, recent work has shown that the response to ozone depletion should be less sea ice, while the opposite is observed (Bitz and Polvani 2012). Moreover, most climate models produce declined Antarctic sea ice in the recent decades (Shu et al. 2015). On the other hand, more recent studies suggest that decadal changes in the Antarctic Peninsular surface climate may be linked to the changes in tropical SSTs (Ding and Steig 2013; Li et al. 2014). These results refocus attention on the connections from the tropics to the poles.

It has been long known that polar climate is strongly influenced by the tropical SST variability related particularly to the El Niño–Southern Oscillation (ENSO) phenomenon, owning to its far-reaching impact on many aspects of the global climate system. The influences of ENSO can be observed in the atmosphere, ocean, sea ice, and glacial ice in polar regions of both hemispheres (Turner 2004). The atmospheric responses at southern high latitudes include anomalies in sea level pressure, troposphere height, streamfunction, blocking events, precipitation, surface winds, and temperature (van Loon and Shea 1985; Mo and White 1985; Krishnamurti, et al. 1986; Trenberth and Shea 1987; Karoly 1989; Smith and Stearns 1993; Cullather et al. 1996; Sinclair et al. 1997; Villalba et al. 1997; Kiladis and Mo 1998; Marshall et al. 1998; Noone et al. 1999; Bromwich et al. 2000; Renwick 1998; Liu et al. 2002). Similarly, the atmospheric responses can be traced in the Northern Hemisphere (NH) extratropics (Trenberth et al. 1998; Pozo-Vázquez et al. 2005; Cassou and Terray 2001; Jevrejeva et al. 2003). The mechanisms fostering the connection between ENSO and the high latitudes through the troposphere include 1) the Rossby waves generated by tropical convection (Karoly 1989; Mo and Higgins 1998; Kiladis and Mo 1998; Garreaud and Battisti 1999); 2) jet stream changes in response to tropical SST changes (Chen et al. 1996; Bals-Elsholz et al. 2001); 3) anomalous mean meridional and zonal circulations and associated heat fluxes (Carleton and Whalley 1988; Cullather et al. 1996; Kreutz et al. 2000; Liu et al. 2002; Seager et al. 2003; Liu et al. 2004; Yuan 2004); and 4) altered transient eddy activity (Carleton and Carpenter 1990; Carleton and Fitch 1993; Sinclair et al. 1997; Carleton and Song 2000). Through the atmospheric connection, ENSO events significantly influence sea ice variability in the Antarctic (Simmonds and Jacka 1995; Yuan and Martinson 2000, 2001; Harangozo 2000; Kwok and Comiso 2002; Martinson and Iannuzzi 2003) and in the Arctic (Gloersen 1995; Loewe and Koslowski 1998; Venegas and Mysak 2000; Jevrejeva et al. 2003).

Studies of the tropical–polar teleconnection have advanced rapidly in the recent decade since earlier reviews on the subject (Trenberth et al. 1998; Turner 2004), given the accumulation of polar cryosphere observations, enhanced atmospheric data assimilation, and improved climate models. Emerging studies suggest that tropical climate variability at other (“non ENSO”) time scales also reaches the polar regions. For example, tropical variability on an intraseasonal time scale, namely, the Madden–Julian oscillation (MJO), impacts extratropical regions as far as the high-latitude Arctic (Yoo et al. 2011). At multidecadal (or long-term trend) time scales, tropical Pacific SST variability and associated Rossby wave trains influence the southern annular mode (SAM) and surface temperature around the AP and West Antarctica (Ding et al. 2011, 2012; Ding and Steig 2013; Schneider et al. 2012a,b; Clem and Fogt 2013, 2015; Clem and Renwick 2015; Yu et al. 2015). The tropical forcing that influences the high latitudes has been also found in the equatorial Atlantic (Li et al. 2014; Simpkins et al. 2014) and Indian Ocean (Nuncio and Yuan 2015). In addition to the connective mechanisms through the troposphere, teleconnections can also take stratospheric pathways (Butler and Polvani 2011). Here, we summarize some of the recent studies, including those mentioned above, which are organized by time scale from intraseasonal, interannual, decadal to multidecadal, and centennial and longer, including paleoclimate studies. In summary, this review tries to follow an overarching theme: that the problems and research findings of recent and past climates can often be appreciated better within the context of tropical–polar linkages. Also, studies of tropical–polar connections based on instrumental records can greatly help paleoclimate researchers better understand inferred processes in the past.

2. Connections at intraseasonal time scales

Tropical–polar teleconnections at intraseasonal time scales were discovered in the last decade. The most profound tropical intraseasonal variability is the MJO, which can modulate high-latitude atmospheric circulation (Matthews and Meredith 2004; Zhou and Miller 2005; Cassou 2008; L’Heureux and Higgins 2008; Flatau and Kim 2013). Based on reanalysis data, satellite observations, polar bottom pressure records, and tide gauge station data, Matthews and Meredith (2004) found that the SAM peaks approximately seven days after the MJO. Three days after this atmospheric response to the MJO, an increase in the ocean transport through Drake Passage was found. This associated oceanic intraseasonal variability is well captured by the Ocean Circulation and Climate Advanced Modelling (OCCAM) global ocean model (Webb and de Cuevas 2002), which indicates that up to 15% of oceanographic intraseasonal variance can be linearly attributed to the

MJO (Matthews and Meredith 2004). On the other hand, Pohl et al. (2010) claimed that the MJO does not have a significant impact on SAM. Contrary to the conclusion of Pohl et al. (2010), Flatau and Kim (2013) found that the MJO is capable of forcing the leading modes of mid–high-latitude atmospheric circulation, namely, the northern annular mode (NAM) and SAM in both hemispheric winter and summer. They showed that Indian (Pacific) Ocean convection related to the MJO precedes the increase (decrease) in the NAM and SAM indices during the respective hemispheric cold seasons. During the hemispheric warm seasons, NAM has a similar response to that in the cold season, but SAM has the opposite response (Fig. 1), although the observational uncertainties are larger for the warm season.

The impact of the MJO on polar atmospheric circulation extends to the surface climate, such as surface temperature. S. Lee et al. (2011) investigated the connection of Arctic temperature variability to MJO using ERA-40 reanalysis data. They used the coupled self-organizing map (SOM) between the NH 250-hPa streamfunction and tropical convective precipitation to detect dynamic links between the low and high latitudes. They found that the tropical convection associated with MJO causes extratropical circulation changes through atmospheric Rossby wave propagation, and the circulation anomalies can be established at high latitudes in 3–6 days as the Pacific–North America (PNA) pattern. These MJO-induced circulation changes alter poleward heat transport. Together with adiabatic warming and downward infrared radiative fluxes, the anomalous poleward heat transport is capable of influencing the variability of winter surface temperature in the Arctic. This result is consistent with the results of Graversen (2006). Yoo et al. (2011) further found in observations that MJO heating in the tropical Pacific is followed 1–2 weeks later by Arctic warming through atmospheric circulation changes [similar to the finding by S. Lee et al. (2011)], whereas MJO heating in the equatorial Indian Ocean is followed by Arctic cooling (Fig. 2).

In addition to the impacts on polar atmospheric circulation, ocean transport, and surface air temperature (SAT), the MJO's influence was also found in Arctic sea ice during both winter and summer (Henderson et al. 2014). Daily sea ice concentration responds to the atmospheric circulation anomaly patterns in high latitudes that are associated with MJO variability. The sea ice responses appear larger in winter than in summer. Although the Arctic sea ice responses are statistically significant, the magnitudes of change are rather small.

New research also has revealed mechanisms by which MJO anomalies affect high-latitude climate. Modeling studies reveal that the MJO influences polar surface

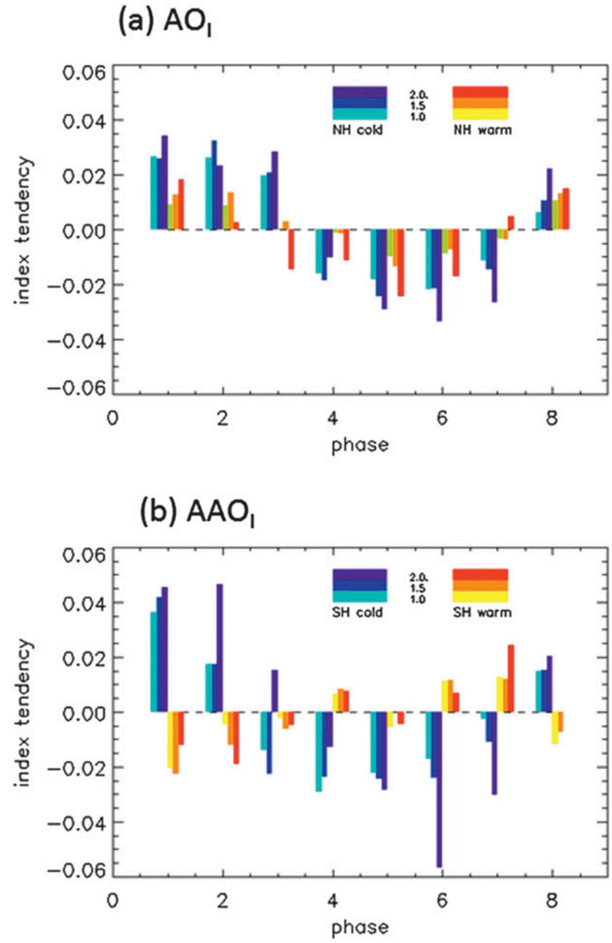

FIG. 1. The average change (tendency) of the index over 1 day for the (a) NAM index and (b) SAM index (gpm day^{-1}). The cool colors denote the changes for the winter cold season, and the warm colors denote the changes for the warm season. The minimum MJO amplitudes considered in the calculation of each average tendency are indicated (Flatau and Kim 2013). MJO phases 1–3 occur in the Indian Ocean and phases 4–8 occur in the Pacific.

temperature through the Rossby wave train propagation (Yoo et al. 2012a,b). Based on a budget analysis of zonal-mean winds, Sakaeda and Roundy (2014) found that the MJO triggers anomalies in the global zonal-mean zonal winds in the upper troposphere at the intraseasonal time scale, starting from the tropics and propagating to the extratropics. The complicated interaction between the background state and zonal-mean zonal winds, as well as the feedback from the modulated synoptic-scale circulation, facilitate the poleward propagation of the MJO-related anomaly.

The Rossby wave propagation and zonal-mean zonal wind changes in the troposphere are not the only mechanisms linking MJO and high-latitude climate. Garfinkel et al. (2012) found that MJO has a strong connection with the NH wintertime stratosphere polar vortex, consequently

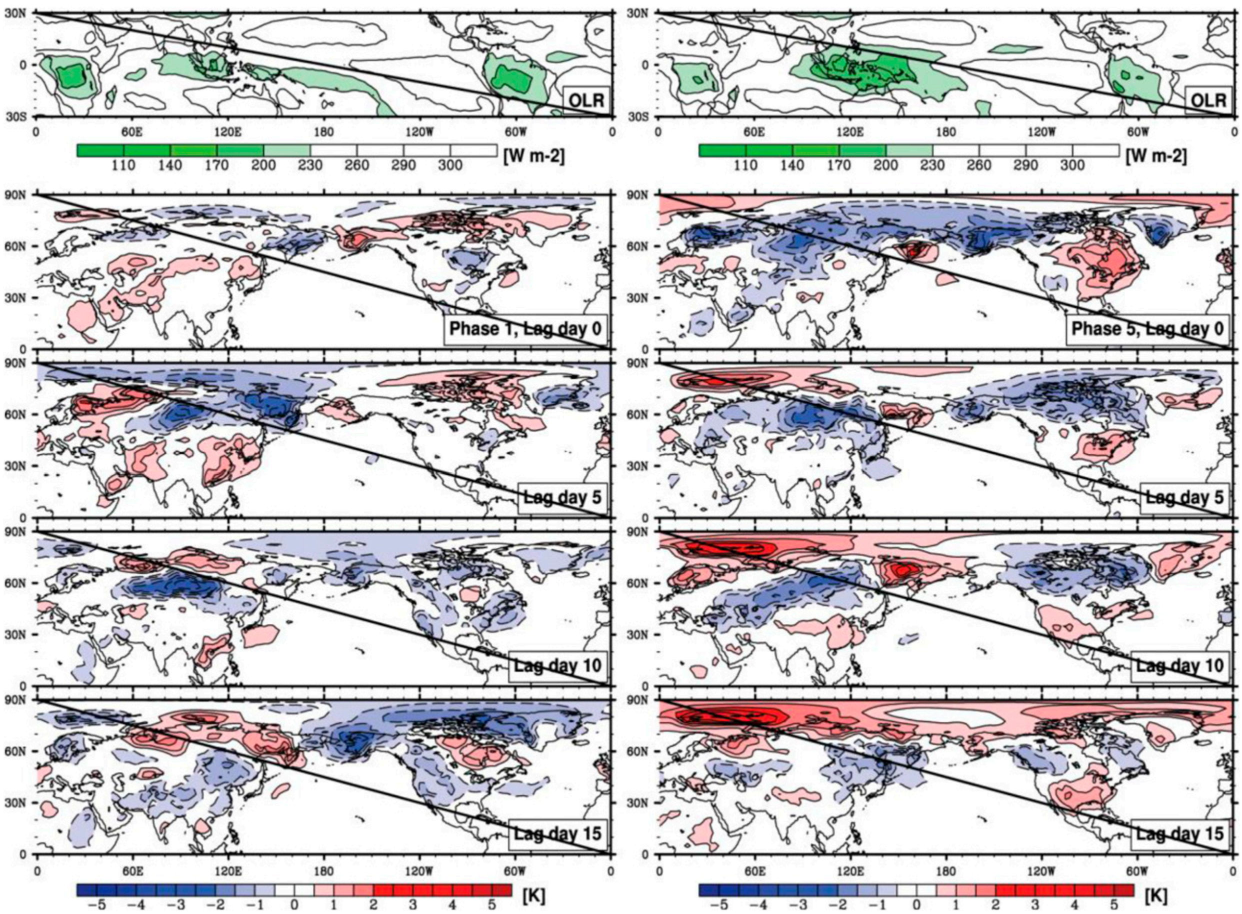

FIG. 2. (top to bottom) Total OLR composite on lag day 0, with lagged composites of SAT on lag days 0, 5, 10, and 15 for MJO phases (left) 1 and (right) 5. The MJO phase 1 is defined when the convection occurs in the western tropical Indian Ocean while MJO phase 5 takes place when the convection occurs in the western tropical Pacific. Solid contours are positive, dashed contours are negative, and the zero contours are omitted (Yoo et al. 2011).

influencing the tropospheric Arctic Oscillation one to two months later. The magnitude of MJO-induced stratosphere temperature anomaly can reach 4 K, which is comparable to that associated with tropical forcing at interannual time scales. The authors hypothesized that MJO-excited Rossby wave trains propagate both poleward and upward, altering the stratospheric polar vortex. Through the downward propagation of stratospheric signal and the coupling between the stratosphere and troposphere, this tropical forcing is then related to the NAM. This stratospheric pathway links the tropical forcing to the polar atmospheric circulation with a longer delay when compared with the Rossby wave connection through the troposphere.

In summary, MJO-associated tropical convection can impact polar atmospheric circulation in both hemispheres, and in both winter and summer seasons. The strong tropical intraseasonal variability propagates to high latitudes within a week. The modulated atmospheric circulation forces the corresponding changes in polar surface air temperature, oceanic transport, and sea ice in as little as a few days to a week. Evidence shows that polar regions respond more strongly to the MJO in hemispheric winter than summer. The mechanism that can explain the connection between the tropics to polar regions is the Rossby wave train propagation in the troposphere, which is supported by both modeling experiments and data diagnostic analyses. The Rossby wave can also disturb the stratosphere and result in a delayed response in the NAM. Also, the MJO-related circulation anomaly in the tropics can propagate poleward in the global zonal-mean zonal winds. Although the connections are identified as statistically significant, MJO-related variability accounts for only 10%–20% of the polar intraseasonal variability, at least in the ocean.

3. Connections at interannual time scales

ENSO is the primary variability in the climate system at the interannual time scale. Its far-reaching impacts on

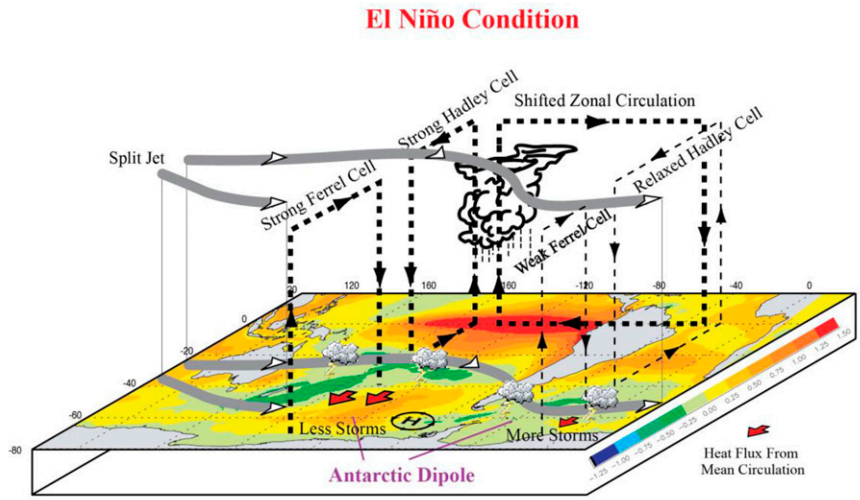

FIG. 3. Schematic atmospheric circulation pattern in response to ENSO warm events superimposed on the corresponding SST composite (Yuan 2004). The Rossby wave train emanating from the tropics leads a high SLP anomaly in the southeast Pacific. Because of the warm SST, the Hadley cell is enhanced and contracted in the South Pacific while weakened and expanded in the South Atlantic. It results in the jet stream moving equatorward in the Pacific but poleward in the Atlantic. This change in the jet stream leads to the changes of storm distribution.

the lower atmosphere, ocean surface, and cryosphere in the polar regions of both hemispheres have been documented in numerous studies and prior review papers (Trenberth et al. 1998; Turner 2004). Advances over the last decade have provided a better understanding of the connecting mechanisms and of different source areas of the tropical forcing and revealed the interactions between low-latitude-induced variability and high-latitude modes of climate variability.

a. The tropics–southern high latitudes connections through the troposphere

In the Southern Ocean, the largest ENSO impacts occur on the surface temperature and sea ice fields, as coherent, large-scale, out-of-phase anomalies between the Pacific and Atlantic sectors of the Antarctic; Yuan and Martinson (2000) termed this pattern the Antarctic dipole (ADP). The ADP anomalies grow into their maximum values in the austral winter following ENSO, by which time the tropical forcing has diminished (Yuan 2004). Yuan (2004) synthesized the mechanisms that link ENSO events to ADP variability, as illustrated in Fig. 3 for the El Niño condition. These mechanisms include 1) Rossby wave trains emanating from the tropical Pacific, leading to an anomalous high pressure center in the Amundsen Sea (weakened Amundsen Sea low); 2) meridional circulations exhibiting zonal asymmetry because of contrasting SST anomalies in the tropical Pacific and tropical Atlantic: the Hadley cell is strengthened and contracted (weakened) in the South Pacific (South Atlantic); 3) equatorward shifting of the subtropical jet and storm tracks in the South Pacific and poleward shifting of storm tracks in the South Atlantic; and 4) an enhanced (weakened) Ferrel cell in the South Pacific (South Atlantic). All of these mechanisms contribute to more poleward heat transport in the lower atmosphere of the South Pacific, and less poleward heat transport in the South Atlantic. These in-phase forcings create long-lasting ADP anomalies in surface temperature and sea ice. La Niña events produce the opposite circulation and ADP anomalies as just described (cf. Fig. 3).

Driven by the Antarctic Circumpolar Current (ACC) and air–sea interactions, some ADP anomalies propagate eastward to form apparent Antarctic Circumpolar Waves. However, the eastward propagation of ENSO signals is interrupted in the Indian Ocean. For example, a recent study found that the ACC's topographic meandering in the south Indian Ocean warms the ocean surface by up to 1°C during winter and reduces sea ice east of 20°E, interrupting the Antarctic Circumpolar Wave propagation (Nuncio et al. 2011).

Recent studies also have advanced further our understanding of the ENSO–Antarctic connection, regarding the asymmetric impacts of El Niño and La Niña (Hitchman and Rogal 2010; Turner et al. 2013) and the different impacts of two types of El Niño events (Wilson et al. 2014, 2016; Yu et al. 2015). Results from these recent studies do not necessarily agree with each other. Examining El Niño and La Niña events separately,

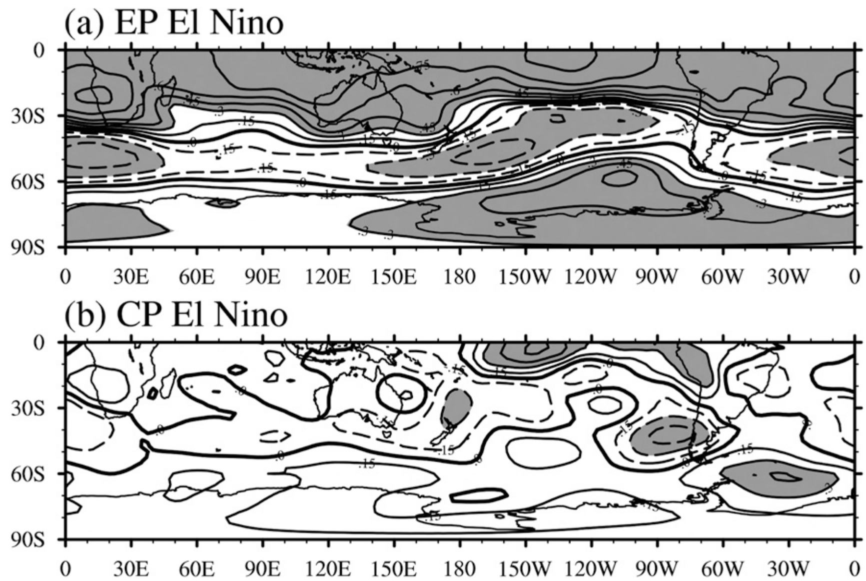

FIG. 4. Partial correlation coefficients of 500-hPa geopotential height (GPH) with the normalized (a) EP and (b) CP El Niño indices for DJF during 1979–2009. The EP El Niño index is defined by the traditional Niño-3 index, while CP El Niño index is defined as $I_{EM} = T_{a,C} - 0.5T_{a,E} - 0.5T_{a,W}$, where $T_{a,C}$, $T_{a,E}$, and $T_{a,W}$ are the mean SST anomalies over the CP (10°S–10°N, 165°E–140°W), EP (15°S–5°N, 110°–70°W), and western Pacific (10°S–20°N, 125°–145°E), respectively. The term I_{EM} reflects the pattern of warm central equatorial Pacific and cold western and eastern equatorial Pacific. Regions above the 90% confidence level are shaded. The Rossby wave train excited by CP El Niño propagates west of the wave emanated by EP El Niño and produces a less significant positive center in the Amundsen Sea (Sun et al. 2013).

Hitchman and Rogal (2010) found that tropical convection shifts westward during La Niña years relative to El Niño years, resulting in a 30°–50° westward shift of the planetary waves in the upper troposphere and lower stratosphere, as well as a westward shift of the ozone column maximum in the southern middle to high latitudes. The tropical signal is communicated to higher latitudes through modulating subtropical anticyclones, which lead to the changes in the location of the column ozone maximum and of the Antarctic polar vortex asymmetry. On the other hand, Turner et al. (2013) disagreed with Hitchman and Rogal (2010) and reported that the depth of the Amundsen Sea low is significantly different between cold and warm ENSO phases for the period of 1979–2008 while the difference in the location of the low was not significant.

Following the identification of central Pacific (CP) El Niño and eastern Pacific (EP) El Niño (Yu and Kao 2007; Kao and Yu 2009), studies have revealed teleconnection differences for different ENSO flavors. Using reanalysis data, Sun et al. (2013) showed that CP El Niño events lead to westward-shifted and localized tropical convection anomalies compared to EP El Niño events, as well as an anomalous Walker cell confined to the central Pacific during boreal winter. The CP El Niño events thus lead to a weaker and northwestward shifting of the Pacific–South America (PSA) pattern compared with EP El Niño events (Fig. 4). Modeling studies (Wilson et al. 2014; Ciasto et al. 2015; Wilson et al. 2016) support this result. For example, Wilson et al. (2014) used the Community Atmosphere Model (CAM) simulations and found that the CP El Niño produces a westward-shifting Rossby wave train over the entire South Pacific, which leads to a shifted Amundsen Sea low and associated ADP anomalies. The shifted Rossby wave train weakens the blockings in the southeast Pacific. Those blocking events are usually associated with EP El Niño.

The responses of southern high latitudes to ENSO events are not only sensitive to different flavors of El Niño, but also sensitive to seasons when the teleconnection occurs. The seasonally changing background circulation affects the energy propagation of atmospheric Rossby waves, as well as their interactions with transient eddies. Based on numerical experiments and observational analyses, Jin and Kirtman (2009, 2010) suggested that the timing of the ENSO response in the extratropics is not solely determined by the peak phase of ENSO, but also by the local seasonality of the NH and SH. They identified austral spring as the strongest

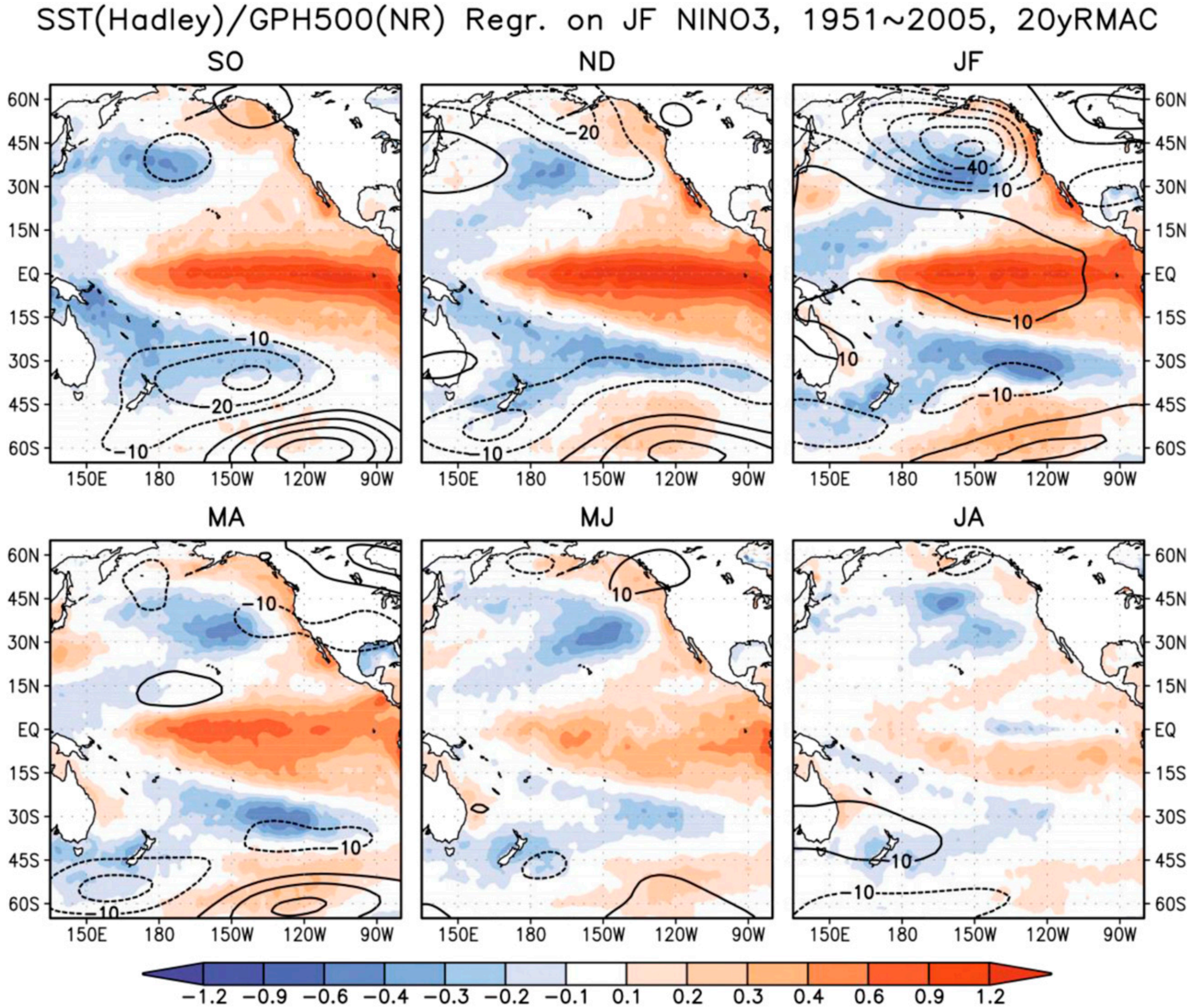

FIG. 5. Regression coefficients of bimonthly SST (°C; shading) and 500-hPa GPH (m; contours) on the Niño-3 index for the period of 1951–2005. SST data are from the Met Office Hadley Centre dataset, and the GPH data are from the NCAR–NCEP reanalysis dataset. The regression coefficients of GPH on the Niño-3 index for the September–October mean time series in the top-left panel show the most profound Rossby wave propagation compared to other months (Jin and Kirtman 2010).

teleconnection season in the SH (Fig. 5). Schneider et al. (2012a) also showed strong seasonality in the Rossby wave train propagation, with the maximum impact on the PSA pattern in austral spring.

Other ENSO–extratropical teleconnection mechanisms, distinct from the Rossby wave train, have also been further developed over roughly the last decade—specifically, a zonally symmetric mechanism, in which tropical heating induces anomalies in the zonal wind in 1) the tropical/subtropical regions through thermal wind balance and in 2) the mid–high latitudes through the eddy-driven mean meridional circulation (Robinson 2002; Seager et al. 2003; L'Heureux and Thompson 2006; Fogt and Bromwich 2006; Fogt et al. 2011; Schneider et al. 2012a). In contrast to the hemispheric seasonality of Rossby wave trains, this mechanism generates extratropical anomalies in both hemispheres simultaneously; therefore, it is less affected by the seasonal variation of the background circulation. This zonally symmetric mechanism extends ENSO signals to mid–high latitudes and influences both the NAM and SAM. Schneider et al. (2012a) found that this mechanism and associated SAM variability can lead to a significant influence on temperature anomalies over eastern Antarctic coastal areas.

ENSO-induced circulation anomalies in high latitudes inevitably interact with regional climate modes, such as the SAM and the wavenumber-3 (wave-3) pattern, and interfere with the natural variability of these modes. These interactions actively modulate ENSO's influence on sea ice and surface climate in Antarctica (Stammerjohn et al. 2008; Yuan and Li 2008; Fogt et al. 2011; Ding et al. 2012; Clem and Fogt 2013; Yu et al. 2015; Wilson et al. 2016). When SAM and ENSO have similar influences on the high-latitude surface climate, it is referred to as ENSO–SAM in-phase, which happens in La Niña/positive SAM years or El Niño/negative SAM years. On the other hand, when the impacts from SAM and ENSO cancel each other, it is referred to as ENSO–SAM out-of-phase, such as La Niña–negative SAM or El Niño–positive SAM years. Studies (Stammerjohn et al. 2008; Fogt et al. 2011) found that the transient momentum fluxes during ENSO–SAM in-phase years reinforce the circulation anomalies in the midlatitudes, resulting in stronger ENSO teleconnections. The ENSO teleconnection is weaker in the ENSO–SAM out-of-phase years. Similarly, the PSA pattern also interacts with wave 3 in the SH. The wave 3 is a quasi-stationary wave pattern around the Southern Ocean in midlatitude pressure and wind fields predominately in winter (Raphael 2004). The anomalous low in the Amundsen Sea low region associated with the La Niña PSA pattern and wave 3's negative pressure anomaly in the area reinforce each other. The interaction produces a stronger branch of the wave-3 pattern in the southeast Pacific (Yuan and Li 2008) and stronger and more consistent La Niña responses in sea ice (Yuan and Martinson 2001). Figure 6 shows significant peaks at 3–5-yr periods in the cross-spectrum analysis of PSA and wave-3 indices, reflecting covariability of these two modes at the interannual time scale.

ENSO's impacts not only appear in the atmospheric circulation, surface climate, and sea ice, but also extend to the deep ocean and under ice shelves. McKee et al. (2011) detected ENSO signals from mooring temperature records at 4560 m below the surface south of South Orkney Island, where bottom water is exported out of the Weddell Sea. ENSO and SAM were mostly in phase from 1997 to 2002, which produced reinforced effects on surface winds, air temperature, and sea ice concentrations in the Weddell Sea shelf region. This enhanced surface forcing produced anomalous shelf water properties, which led to anomalous bottom water formation. After shelf water was formed and exported off the continental shelf and transported out of the Weddell Sea by the gyre circulation, the variability of the Weddell Sea Bottom Water properties at the mooring site were found to lag ENSO, SAM, and surface ADP signals by 14–20 months (Fig. 7). Dutrieux et al. (2014) reported that the strong 2012 La Niña event was linked to the deeper Amundsen Sea low (easterly wind anomaly near the shelf break) that led to a weaker Circumpolar Deep Water (CDW) intrusion in the Pine Island Bay, resulting in a lower ocean temperature under the Pine Island Ice Shelf. Consequently, the ice shelf basal melt in 2012 was reduced by 50% relative to that previously in 2010.

Recent studies also suggest that the heating in the tropical Pacific is not the only forcing of tropical–polar connections. The tropical Atlantic and North Atlantic were also identified as source regions that influence southern high latitudes at interannual and longer time scales (Li et al. 2014; Simpkins et al. 2014). In addition, Nuncio and Yuan (2015) found that the tropical SST associated with the Indian dipole also emanates Rossby wave trains, which then propagate toward southern high latitudes. The Indian dipole often coexists with ENSO events and the joined tropical forcing leads to a merged Rossby wave train in the South Pacific region, affecting sea ice in the southeast Pacific. When the Indian dipole occurs without ENSO events, the Rossby wave train emanating from the tropical Indian Ocean propagates farther south in the southern Indian Ocean and impacts the sea ice field in East Antarctica.

b. *ENSO teleconnection through the stratosphere*

Although many studies attribute the tropically excited Rossby wave trains in the troposphere as a key mechanism connecting the tropics to both polar regions, some recent investigations also suggest an ENSO teleconnection through the stratosphere, similar to the MJO stratosphere connection to high polar regions (Bell et al. 2009; Ineson and Scaife 2009; Ortiz Beviá et al. 2010; Butler et al. 2014). Using the Met Office Hadley Centre atmospheric model with 60 levels in the vertical, Ineson and Scaife (2009) found that the stratosphere plays an important role in connecting El Niño events and the surface climate across northern Europe. During the years when stratosphere sudden warming (SSW) events occur, the Rossby wave associated with El Niño events can propagate upward and disturb the stratosphere in a wave-1 pattern. The abnormal stratosphere signal then propagates down to the troposphere at monthly time scales, producing colder temperatures in northern Europe and warmer temperatures in Canada. This stratosphere pathway appears inconsistent when SSW events are absent (an inactive stratosphere). Moreover, this pathway is highly nonlinear. The number of SSW events is doubled during both El Niño and La Niña years compared with ENSO-neutral years (Butler and Polvani 2011). Further, Butler et al. (2014) found that through the stratospheric path, both warm and cold ENSO events produce the negative NAO circulation pattern, resulting in cold winters over Eurasia and warm winters in eastern Canada and Greenland. This connection only

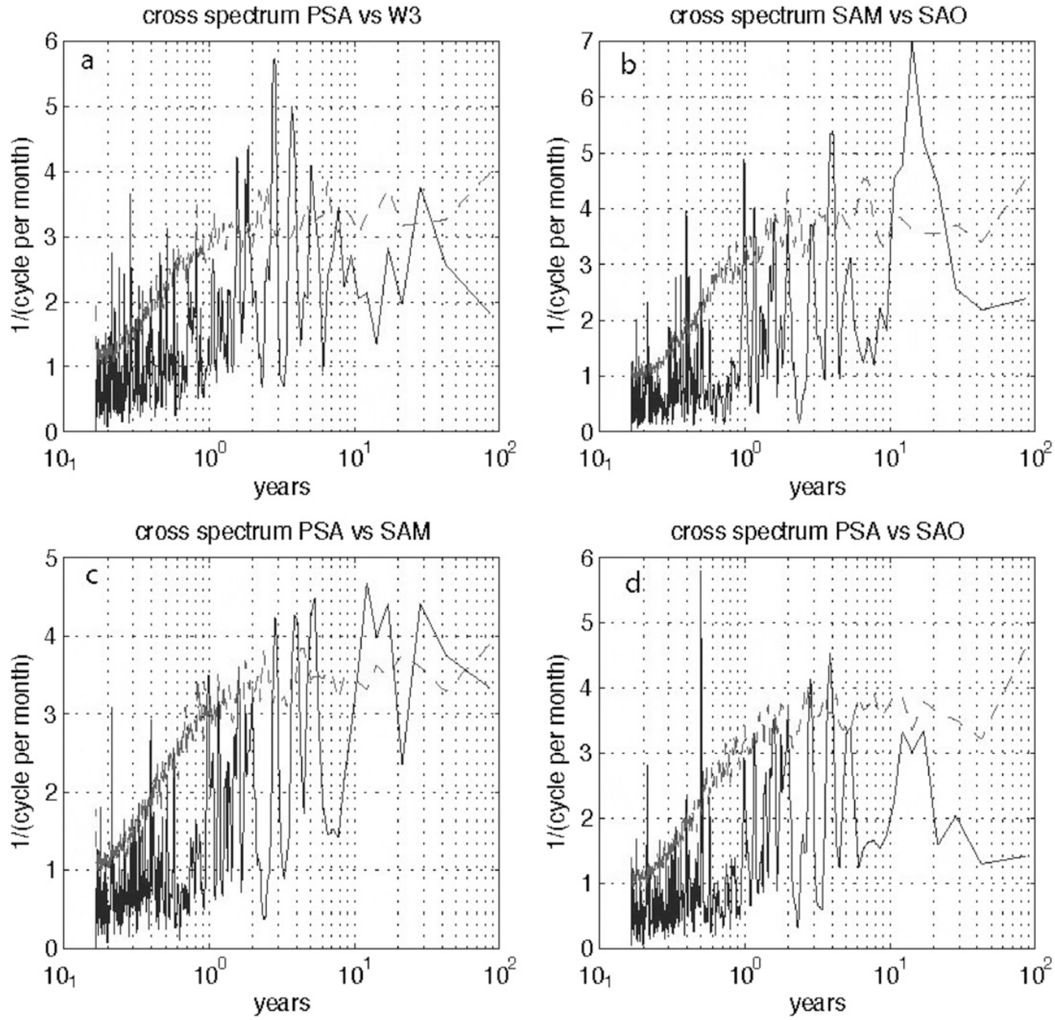

FIG. 6. Cross-spectra between (a) PSA and wave 3, (b) SAM and semiannual oscillation (SAO), (c) PSA and SAM, and (d) PSA and SAO. SAO is an index of semiannual oscillation defined as the difference between zonal-mean SLP at 50° and 65°S. The 53-yr (1950–2003) monthly time series of these indices derived from NCAR–NCEP reanalysis were standardized and detrended before calculating the cross-spectra. Dashed lines indicate the 95% confidence level. PSA and wave 3 share significant energy at 3–5-yr periods. SAM and PSA also share significant variance at interannual and decadal time scales (Yuan and Li 2008).

occurs during winters when the stratosphere is severely perturbed (e.g., with large numbers of SSW events; Fig. 8).

4. Connections at decadal to multidecadal time scales

Limited available observational records confound the assessments of multidecadal variability in the climate system and associated linkages between the tropics and polar regions. Therefore, research on teleconnections at decadal to multidecadal time scales has primarily focused on long-term linear trends in the instrumental data period, including that observed for temperature. In the SH, the strongest warming trend has occurred across the AP region from austral fall to spring and throughout West Antarctica during austral spring (Schneider et al. 2012b; Bromwich et al. 2013; Ding and Steig 2013; Nicolas and Bromwich 2014), while temperature changes appear insignificant in East Antarctica. Early studies attributed the significant AP warming to the long-term sea ice retreat in the Bellingshausen Sea and Amundsen Sea. In contrast, recent studies (Fogt and Bromwich 2006; Steig et al. 2012; Okumura et al. 2012; Ding et al. 2011, 2012; Ding and Steig 2013; Schneider et al. 2012b; Simpkins et al. 2014; Li et al. 2014; Clem and Fogt 2015; Clem and Renwick 2015) indicate that the rapid warming over the last few decades around the AP and West

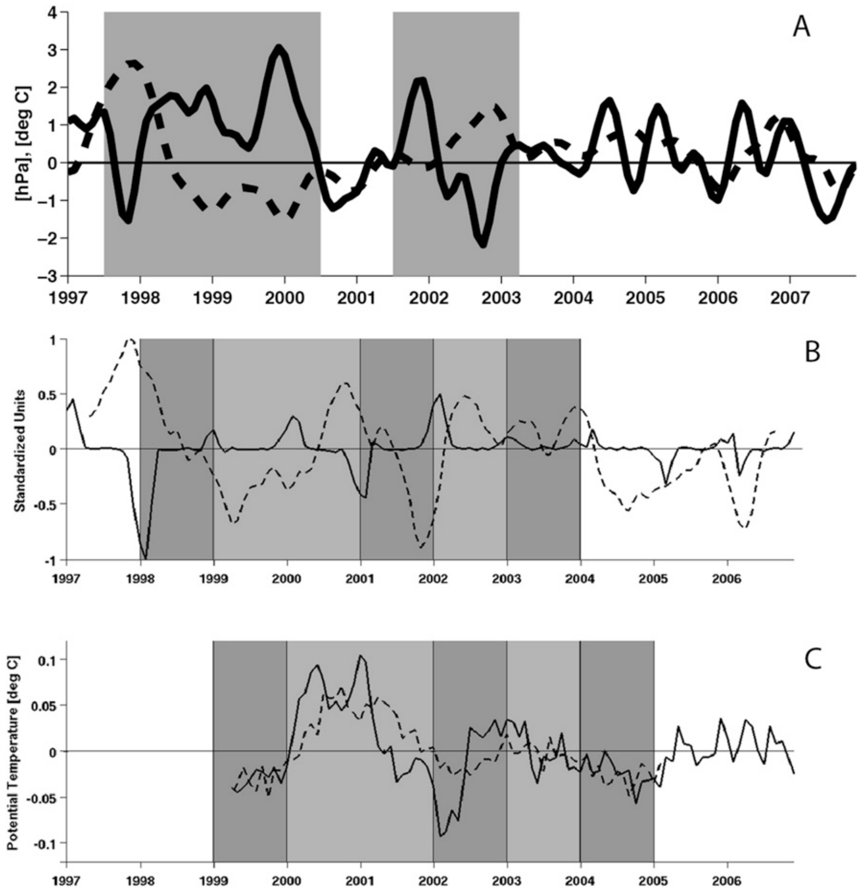

FIG. 7. (a) SAM (solid) and Niño-3.4 (dashed) indices from 1997 to 2007. The indices' out-of-phase periods, which produce in-phase impact in the Weddell Sea, are shaded in gray. (b) Six-month running mean of meridional wind anomalies (dashed line) at 75°S, 52.5°W, and SIC anomalies averaged over the shelf in the western Weddell Sea (solid). Dark gray shading marks calendar years when more shelf water is formed, while light gray shading marks years when less is formed. (c) Temperature anomalies at 3096 m (dashed line) and 4560 m (solid line) below sea surface in the northwest Weddell Sea. The dark gray shading indicates calendar years of anomalously cold pulses, and light gray indicates calendar years of anomalously warm pulses (mean temperature anomaly for that year, negative or positive, respectively). Negative SAM and El Niño events lead to more shelf water production in the western Weddell Sea shelf region, and consequently produce cold pulses on the Weddell Sea Bottom Water more than a year later (McKee et al. 2011).

Antarctica originated from tropical regions. The high-latitude warming was commonly related to an SST pattern of warming in the western tropical Pacific and cooling in the central and eastern tropical Pacific (Fig. 9a). This La Niña–like SST trend pattern also appears in the tropical SST anomalies during the negative phase of the Pacific decadal oscillation (PDO) and the negative phase of the interdecadal Pacific oscillation (IPO). The Rossby wave train associated with this tropical Pacific SST long-term change still primarily connects the tropics to high latitudes at this time scale, resulting in a deepening of the Amundsen Sea low (Fig. 9c) and warming in AP and West Antarctica. However, a variety of Rossby wave flavors, possible source regions of the tropical forcing, and the preferred connecting seasons have been proposed to infer the teleconnection to high latitudes.

Ding and Steig (2013) gave a good example of this SST linear trend pattern in the tropical Pacific and the co-existing deepening of the Amundsen Sea low during the last three decades (Fig. 9). They related these long-term trends in SST and SH pressure field to the widespread warming in AP during austral fall through the Rossby wave train connection. On the other hand, West Antarctica surface temperature has the most significant warming trend in austral winter and spring (Ding et al.

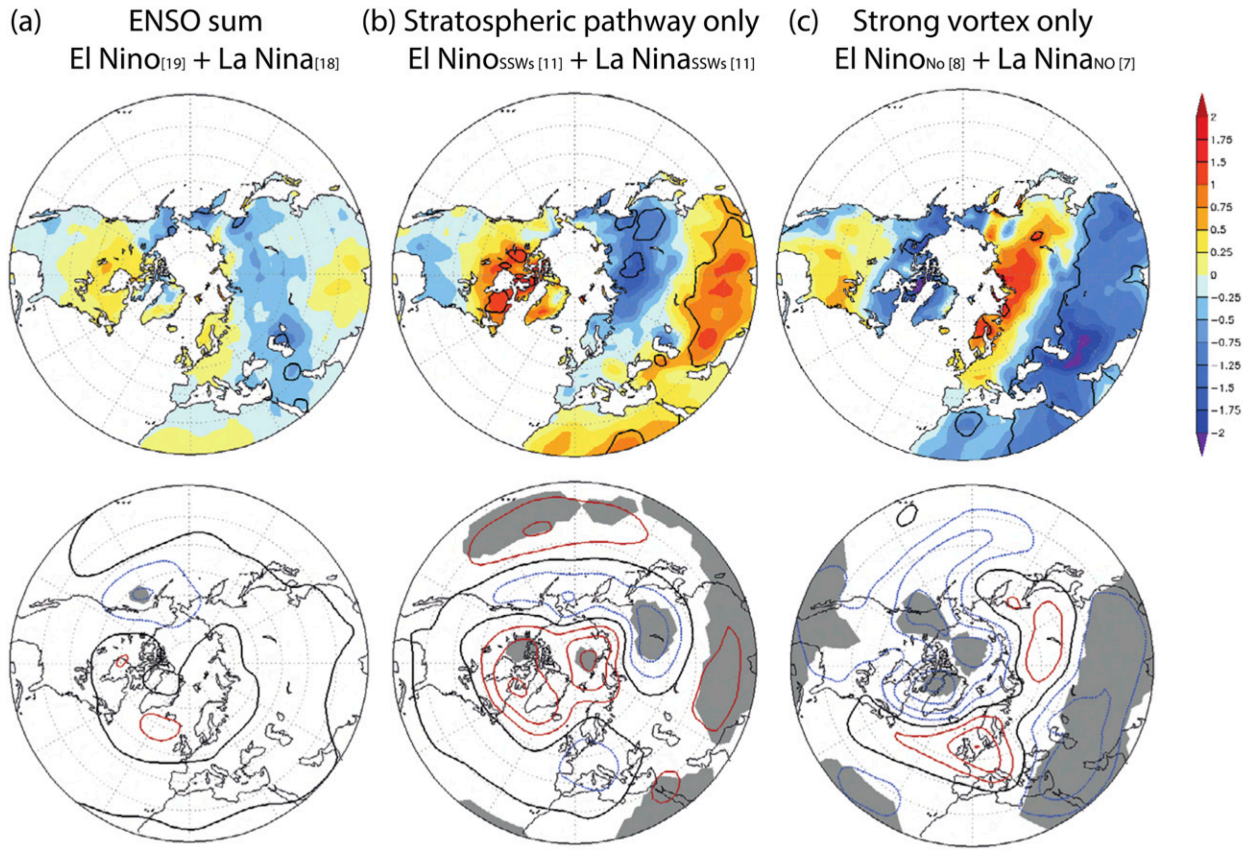

FIG. 8. (top) Surface temperature (K, color shading), and (bottom) 500-hPa GPH (gpm; contour interval 10 gpm) anomalies associated with the composite sum of (a) all El Niño and La Niña winters, (b) El Niño and La Niña winters in which at least one SSW occurs, and (c) El Niño and La Niña winters during which no SSWs occur. In the bottom panels, the red (blue) contours indicate positive (negative) GPH anomalies, and the black line (gray shading) indicates anomalies with $p < 0.05$ for a two-tailed Student's t test. The composites were calculated from the NCAR–NCEP reanalysis dataset for the period of 1958–2013. The mean for all ENSO events in (a) cancels the linear impacts induced by El Niño and La Niña events. The composites of ENSO events with SSWs in (b) limit ENSO's linear influence in the troposphere (no clear Rossby wave in the GPH composite) and isolate ENSO's influence through the stratospheric pathway, which results in a warm North American and cold Europe. Without ENSO influences, the stratospheric activity produces the opposite temperature anomalies in (c) (Butler et al. 2014).

2011; Schneider et al. 2012b; Bromwich et al. 2013). Ding and Steig (2013) suggest that the persistence of the fall sea ice anomaly into the following winter and spring leads to warmer air temperature over the western AP and West Antarctica for all three seasons. Indeed, Schneider et al. (2012b) showed that the sea ice long-term retreat in the Bellingshausen and Amundsen Seas could account for at least 50% of the spring warming in West Antarctica and a significant portion of the spring warming in AP during 1979–2008. Moreover, Clem and Fogt (2015) directly related the similar La Niña–like SST pattern and associated PSA pattern to the spring warming in the western AP. They further distinguish the La Niña–like tropical SST forcing from the negative PDO pattern in the tropics. The negative PDO phase after the late 1990s tends to propagate the Rossby wave more meridionally across the South Pacific and results in a deeper and westward-shifted Amundsen Sea low, which is more closely tied to the widespread warming in West Antarctica (Clem and Fogt 2015). On the other hand, Meehl et al. (2016) recently reported that the recent sea ice expansion in the Ross Sea is mainly driven by the cooling in the eastern tropical Pacific since 2000, which is associated with the negative phase of IPO. One exception to the La Niña–like SST trends in the tropics is that the long-term warming in the central equatorial Pacific is related to the warming of western West Antarctica in austral winter. Again, the Rossby wave train facilitates the connection and results in a high-pressure anomaly center in the Amundsen Sea. Consequently, the surface warming is limited to an isolated area in western West Antarctica (Ding et al. 2011). These studies show that long-term changes in the equatorial Pacific SST have different flavors in different seasons, which result in

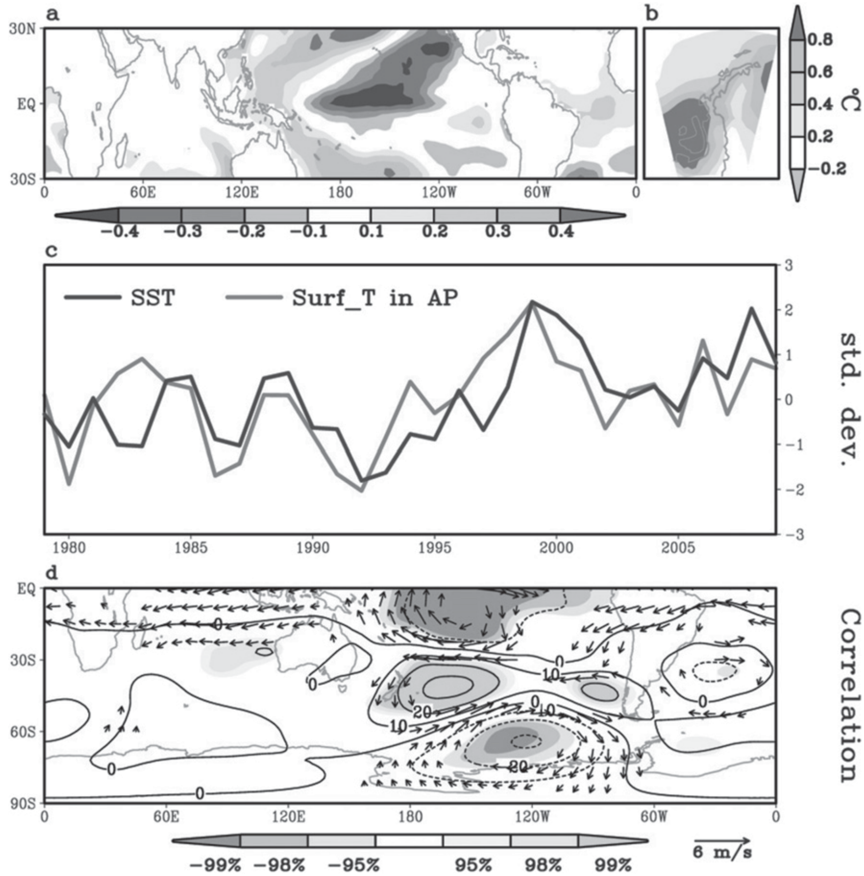

FIG. 9. Principal modes of covarying tropical SST and AP surface temperature in austral fall. Maximum covariance analysis (MCA) results for MAM 1979–2009 tropical (30°S–30°N) SST and surface air temperature in the AP. (a) Mode 1 tropical SST (shading interval 0.1°C) and (b) mode 1 surface temperature in the AP (shading interval 0.2°C). (c) Mode 1 expansion coefficient of the SST (dark gray) and surface air temperature in the AP (light gray). (d) Regression of the MCA mode 1 SST times series against ERA-Interim geopotential height (contour interval of 10 m) and winds (vector; m s^{-1}) at 200 hPa. Amplitudes in (a) and (b) are scaled by one standard deviation of the corresponding time series in (c). In (d), shading denotes regions in which the correlation of the MCA mode 1 SST time series with Z200 is significant at or above the 95% confidence level. The wind vectors are displayed if either component is significantly related to the MCA mode 1 SST time series (above the 95% confidence level) (Ding and Steig 2013).

various kinds of Rossby wave trains and link to different surface climate trends in Antarctica. It is worth mentioning that the confidence levels of linear trends depend on the length of time series and ending points. Reliability of the above-suggested teleconnections is subject to the time series used in these studies. The differences among these studies may also arise from using data in different periods.

Although past research identified the tropical Pacific as a primary source region for the teleconnection, new studies reveal that the tropical Atlantic also influences polar regions through the Rossby wave mechanism (Li et al. 2014; Simpkins et al. 2014). For example, Li et al. (2014) found that the Amundsen Sea low strengthens during the positive phase of the Atlantic multidecadal oscillation, warming the surface temperature and decreasing sea ice in the AP–Weddell Sea sector. Their results were supported by GFDL atmospheric model experiments (Simpkins et al. 2014). Simpkins et al. (2014) also pointed out that the long-term trend in tropical Atlantic SST over the last few decades is likely associated with the trends in the extratropical atmospheric circulation, which have led to the warming around the AP and West Antarctica.

Another noticeable long-term change in the SH is the positive trend in westerly wind strength. Schneider et al. (2015) found that during the last three decades the trend of westerlies in the Pacific sector is 3 times the zonal-mean trend related to the increase of SAM. While the SAM-related zonal-mean trend reaches its maximum in

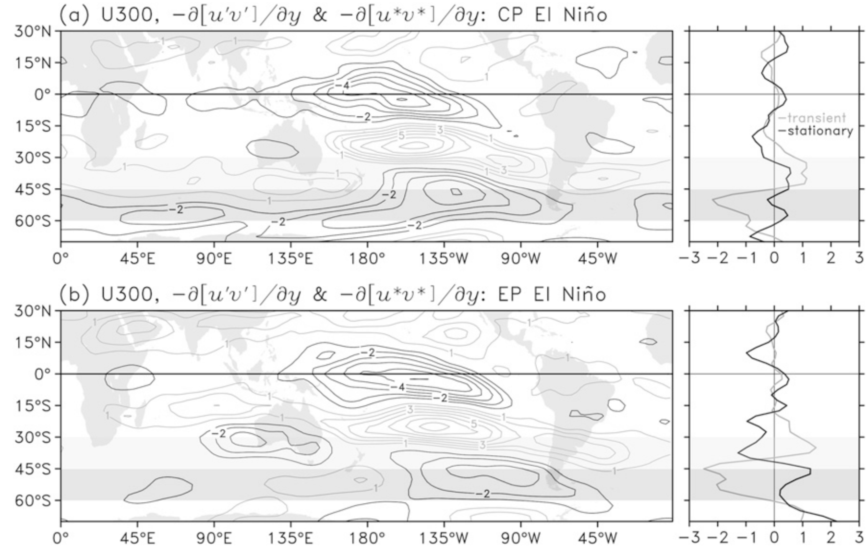

FIG. 10. (left) Composite 300-hPa zonal wind anomalies ($m\,s^{-1}$) and (right) transient eddy momentum flux convergence ($10^{-6}\,m\,s^{-2}$; gray lines) and stationary eddy momentum flux convergence ($10^{-6}\,m\,s^{-2}$; black lines) for the (a) CP El Niño and (b) EP El Niño events. Light (dark) gray shading indicates the equatorward (poleward) side of the midlatitude jet. The zonal winds and momentum fluxes are derived from the NCEP–NCAR reanalysis dataset for the period of 1979–2014. The transient eddy momentum convergence and stationary momentum convergence cancel each other out in the mid–high latitudes for EP El Niño events, resulting in a weaker high-latitude ENSO impact (Yu et al. 2015).

austral summer, the Pacific regional westerly trend is maximized in austral autumn. Although many studies attributed SAM's positive trend to ozone depletion (Thompson and Solomon 2002; Thompson et al. 2011; Previdi and Polvani 2014), the regional trend in winds can be partially attributed to tropical SST changes through the Rossby wave mechanism at multidecadal time scales. Furthermore, the increase of regional westerlies in austral autumn, particularly beginning in the early 1990s, drove an increase in Circumpolar Deep Water intrusions onto the Amundsen Sea shelf, which increased the oceanic heat available for melting of ice shelves (Steig et al. 2012).

In addition to the above-mentioned long-term changes in the tropics, the interaction between high-latitude responses to the tropical forcing and SAM has also changed because of the change in the high-latitude mean state, which in turn leads to the trends in sea ice and surface climate in the Antarctic during the recent decades. Because SAM has become more positive since the early 1990s (Stammerjohn et al. 2008; Clem and Fogt 2013; Yu et al. 2015), the ENSO–SAM in-phase, particularly the La Niña and positive SAM combination, prevails in the 1990s but does not in the 1980s (Stammerjohn et al. 2008). Positive SAM and La Niña have reinforced each other to transport heat poleward and to favor ice reduction in the Bellingshausen Sea and west of the AP. That leads to sea ice retreating earlier and advancing later in the Bellingshausen Sea and west of the AP, resulting in almost a three-month-shorter ice season during the period of 1979–2004 (Stammerjohn et al. 2008). Yu et al. (2015) agreed with Stammerjohn et al. (2008) that ENSO and SAM are more in phase after the 1990s. They attributed this to more CP ENSO events in the recent decades, which not only emanate Rossby waves toward high latitudes but also contribute to the positive trend in SAM. They suggested two mechanisms that link CP ENSO to SAM: one is through the eddy mean–flow interaction mechanism in the troposphere proposed by Seager et al. (2003), as shown in Fig. 10, and the other is a planetary wave in the stratosphere (Hurwitz et al. 2011, 2013; Zubiaurre and Calvo 2012). Clem and Fogt (2013) also noticed that SOI–SAM correlations change sign from the 1980s to 1990s. However, they cautioned that the change is likely dictated by the relatively brief 1988/89 La Niña and negative SAM event, instead of a persistent decadal change.

In the NH, rapid Arctic warming and sea ice retreat signify the polar amplification of anthropogenic climate change. The most profound warming in annual-mean surface and tropospheric temperature has occurred in northeast Canada, Greenland, and northern Siberia during the last three decades (Ding et al. 2014). The scientific community has debated the relative roles of local factors, such as the albedo effect, versus a remote forcing in driving the amplified Arctic warming. Based on forced AGCM experiments, Screen et al. (2012) suggested that the trends in sea ice concentration and SST explain a significant portion of the near-surface warming, while the tropical SST trends contribute to the majority of upper-tropospheric warming. Other studies (S. Lee et al. 2011; Ding et al. 2014) attributed the Arctic surface warming to the long-term changes of Rossby wave trains initialized in the tropics at intraseasonal to interannual time scales. Based on observational data and forced model experiments, Ding et al. (2014) showed that the rapid warming in northeast Canada and Greenland is related to the negative trend in the North Atlantic Oscillation, which is associated with the Rossby wave train triggered by tropical Pacific SST. In particular, the warming cannot be explained in the model experiments by prescribed anthropogenic forcing, suggesting that the tropics are likely a forcing for at least a portion of the warming in the region.

As discussed in section 2, the tropical convection associated with the MJO is the source of Rossby wave trains that propagate to high latitudes in both hemispheres. It has been suggested that the decadal and multidecadal changes in MJO contribute to long-term temperature trends in the Arctic (Yoo et al. 2013, 2013; Lee 2012) and Antarctic (Yoo et al. 2012c). In the NH, the occurrence of MJO convection has increased in the western tropical Pacific during 1979–2008 (Yoo et al. 2011), which is likely caused by the above-mentioned long-term warming in the region. As discussed in section 2, MJO convection in the western tropical Pacific is associated with poleward heat transport to the Arctic through the Rossby wave connection. Consequently, this multidecadal change in the MJO convection has contributed to recently accelerated Arctic warming. The MJO-induced temperature trend accounts for 10%–20% of the observed hemispheric winter warming in the Arctic (Yoo et al. 2011) and Antarctic (Yoo et al. 2012c), which may be only a small fraction of total tropical-related warming, particularly in the SH.

5. Inferred connections in past climates

In this section, we focus on inferred teleconnections based on proxy data and model experiments since the last Ice Age or global Last Glacial Maximum (LGM; i.e., since about ~18 000 years ago), although many of the findings and inferences discussed are relevant also for deeper time periods. We acknowledge that earlier time periods can inform our understanding of tropical–polar connections (e.g., Molnar and Cane 2007; Chiang 2009; IPCC 2013; Ford et al. 2015).

a. Evidence for tropical impacts on higher latitudes

Tropical teleconnections evident in the instrumental record provide essential lessons for understanding past connections with the high latitudes. As discussed above, warm SSTs in the tropical Pacific can generate an atmospheric Rossby wave response that propagates to high latitudes, and also can create zonally symmetric responses in subtropical jets and westerlies in both the NH and SH. By implication, ENSO must feature prominently in past tropical–high-latitude linkages, given its worldwide importance in climate variability on the interannual, decadal, and multidecadal time scales (e.g., Turner 2004; Chiang 2009; Mayewski et al. 2009). Here we mention studies that have inferred past ENSO teleconnections with the high latitudes since the last Ice Age.

Turner (2004) provided a comprehensive review of observations and modeling results for past ENSO signals at high southern latitudes, although he highlighted that the mechanistic (including theoretical) routes to the polar regions are often less clear and (still) remain poorly understood. Since Turner (2004), paleoclimate studies have continued to document ENSO-like signals and hypothesized effects at the high latitudes of both hemispheres, including how it may have interfered with the phase of the SAM in a nonlinear way (sections 3 and 4; Turner 2004; Stammerjohn et al. 2008; Clem and Fogt 2013). Because of dating or proxy resolution, paleostudies must focus on ENSO-like changes in terms of systematic trends or variance over the centennial (or longer) time scale (e.g., Meyerson et al. 2002; Villalba et al. 2005; Villalba 2007; Mayewski et al. 2009; Barron and Anderson 2011; Clegg et al. 2011; Ford et al. 2015). In NH high latitudes, studies have used evidence from North America to document the global effects of past tropical ENSO-like variability (e.g., Barron and Anderson 2011; Clegg et al. 2011). Likewise, in SH higher latitudes, studies have also continued to reconstruct the global influence of tropical ENSO-like variability (Meyerson et al. 2002; Villalba et al. 2005; Villalba 2007; Mayewski et al. 2009). Specifically, these and other studies documented relatively weak ENSO variance in the early–middle Holocene (~11 500 to ~5000 yr ago; Moy et al. 2002; Koutavas and Joanides 2012; Carré et al. 2014), which may have corresponded with persistently positive SAM-like scenarios, as reflected in pervasive warm and dry conditions for the higher (sub-Antarctic) latitudes of Patagonia (Moreno and Videla 2016; Kaplan et al. 2016). Conversely, strong ENSO variance in sub-Antarctic Patagonia and negative SAM-like states during the late Holocene (last ~5000 yr) appear to be reflected by cold and wet periods (Moreno et al. 2014). In the present climate, the amplitudes of ENSO can be influenced by the mean state of the tropical Pacific (Choi et al. 2009; Kang et al. 2015). The change of the tropical mean state can be generated from an internal process of the tropical Pacific such as asymmetric ENSO events (Timmermann 2003; Rodgers et al. 2004; Dewitte et al. 2007; Sun and Yu 2009). Choi et al. (2009) linked the warmed mean tropical Pacific SST to the amplification of ENSO variability by the internal positive feedback between these two. Similarly, Kang et al. (2015) found that the lower ENSO amplitude is associated with the cooling of the central tropical Pacific. In turn, some climate models suggest that higher ENSO amplitudes strengthen the relationship between ENSO and SAM (Cai et al. 2011). We infer that such relationships existed in the past, including (internal) tropical Pacific feedbacks that affect ENSO amplitude, which in turn are linked with SAM strength. However, as implied by Turner (2004), the dynamical mechanisms linking long-term (i.e., paleo) changes in the ENSO amplitude and the SAM phase remain poorly understood.

At the highest latitudes (e.g., >40°S) of southernmost South America, some studies of the most recent Holocene (last ~1000 years) climate noted that no significant correlations can be detected between tropical climatic drivers and tree growth (Villalba 2007; Moy et al. 2009; Villalba et al. 2005, 2012); these researchers found instead a relatively stronger polar influence on temperatures and precipitation over the southernmost part of the continent. However, tree ring records are limited mainly to the last ~500 years, and the relative strength of the tropical influences on the higher latitudes of southern South America may have been stronger prior to the last few centuries, especially during warm phases such as in the early Holocene (e.g., from ~11 500 to 8000 years ago).

The middle Holocene may be a time when important changes occurred in the tropics, including ENSO variability, and associated changes should be evident in the polar regions (Fig. 3) (cf. Turner 2004). Most reconstructions of ENSO show notable shifts around the middle Holocene, with a modern regime being recognized by the mid–late part of the epoch (e.g., Moy et al. 2002; Koutavas and Joanides 2012; Carré et al. 2014). However it should be noted that, based on coral data, Cobb et al. (2013) inferred highly variable ENSO activity with no evidence for a systematic trend over the last 7000 years. Interestingly, middle-to-late Holocene cooling and the onset of Holocene mountain advances are also documented in the middle–high latitudes of the Northern and Southern Hemispheres (e.g., Solomina et al. 2015).

Studies have also focused on the initial or external forcing of tropical climates and the consequences for connections with the high latitudes. Observations and modeling studies indicate past tropical to polar climate connections would be affected by changes in low-latitude irradiance and orbitally driven forcing of the seasonal cycle of solar radiation (e.g., because of the precession of the equinoxes; Cane et al. 2006). Emile-Geay et al. (2007) suggested that in the past, ENSO variability was a mediator between the sun and high-latitude climate changes. A focus has been on the early and middle Holocene when incident solar radiation during boreal summer was stronger than today (a July perihelion; e.g., Clement et al. 2000; Cane et al. 2006; Emile-Geay et al. 2007). Models show this change in the seasonal cycle causes both the eastern and western equatorial Pacific to respond. However, because the SST in the western tropical Pacific is thermodynamically determined while upwelling in the east influences SST, the ocean response to this uniform insolation change is additional warming of the west side of the tropical Pacific. The east–west contrast creates a deeper low on the west side of the low-latitude Pacific where atmospheric convergence and ascent occurs, and a cooler east side, which is conducive to weaker ENSO variability that is indeed observed in some datasets mentioned above.

Emile-Geay et al. (2007) also argued that Asian–Indian monsoons should mediate the connection between the tropical Pacific and higher latitudes in the North Atlantic. Increased solar irradiance and warming of the western equatorial Pacific, more than the east, may be conducive to strengthening of the monsoons, enabling a more positive phase of the NAO. In contrast, decreased irradiance may foster persistent El Niño–like SST anomalies, which play a role in a weakened Asian monsoon, northeasterly winds around the Fram and Denmark Straits, and a regional climate pattern resembling a negative NAO. Furthermore, Emile-Geay et al. (2007) inferred that such ENSO-induced perturbations in the North Atlantic, involving sea ice and the thermohaline circulation, would then reverberate back into the tropical Pacific, further intensifying the El Niño–like anomaly in a positive feedback, leading to even colder Arctic temperatures (negative NAO).

The discussion so far has focused on the current interglacial period. On longer glacial to interglacial time scales, the tropical latitudes may have an important (indirect) impact on high-latitude climates through changes in greenhouse gases, including atmospheric methane (CH_4) and water vapor. A high-resolution record of CH_4 was recently obtained from an annually dated Antarctic ice core on the West Antarctic Ice Sheet (WAIS) Divide, building on prior work in Greenland (Buizert et al. 2015). Changes in tropical biosystems, specifically in the Neotropics and Southeast Asia, are a reasonable smoking gun for major CH_4 variations prior to humans (Mitchell et al. 2013; Sjögersten et al. 2014). In addition, during Ice Age climates, decreased water vapor content and relative humidity in the tropics led to additional low-latitude and global cooling (PALAEOSENS Project Members 2012). Seager et al. (2000) found that reducing the relative humidity of the entire troposphere (above the subcloud layer) by 10%–20% cools tropical SST by about 2 K.

b. Evidence for polar feedback to the tropics

This section so far has primarily focused on the tropical influence to high latitudes. Because of the larger ice sheet and sea ice extent during Ice Age climates, it is important to examine the influence of polar regions to lower latitudes in paleorecords. There is a vast literature that explains how, during Ice Age climates, high-latitude NH ice sheets and extensive sea ice coverage in both hemispheres could have impacted the tropics, through both direct (radiative) and indirect effects (e.g., Chiang and Bitz 2005; Chiang 2009; PALAEOSENS Project Members 2012; Chiang et al. 2014; Lee et al. 2015; Figs. 11–13). Observational and modeling-based studies have examined polar to tropical communications at a range of time scales from orbital to suborbital (e.g., PALAEOSENS Project Members 2012; IPCC 2013).

A basic reason why polar climates strongly influenced the tropical latitudes during cold climates, such as during Ice Ages, is that the high- to low-latitude temperature gradient was greater; hence, polar amplification of climate change would have been particularly important during such climates (PALAEOSENS Project Members 2012; IPCC 2013; Lee et al. 2015). The largest air and sea surface temperature changes obviously occurred in the polar regions, with declines in some areas much greater than 12 K (Fig. 11; Cane et al. 2006; PALAEOSENS Project Members 2012). Whereas global "mean" surface air temperature was likely reduced by ~5–6 K, in most places tropical (30°S–30°N) temperatures may have been only reduced by an average of ~3–2 K, although the amount of tropical temperature depression would have spatially varied (Fig. 11b).

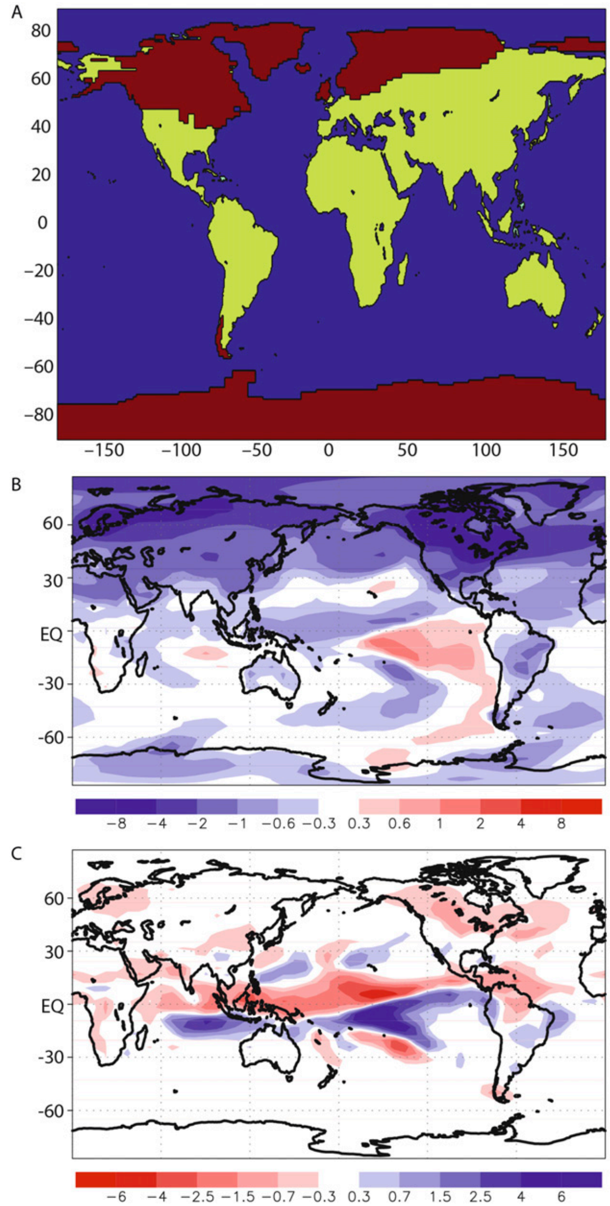

FIG. 11. During the last Ice Age or LGM, there were marked changes in temperature and precipitation relative to the present. As an example, the changes shown here are from Chiang and Bitz (2005), who used the CCM3 coupled to a 50-m slab ocean to study this period. (a) The described glacier extent (red) during the LGM. Glacier ice covered large tracts of the high (and even middle) latitudes; (b) annual-mean differences in SST and surface temperature between LGM and present-day simulations; (c) annual-mean differences in precipitation (mm day^{-1}) between LGM and present-day simulations. Note the southward shift of the ITCZ across the globe and the marked consequential shift in precipitation patterns.

A polar to tropical connection would have been through advection, whereby the large NH ice sheets caused cooling and drying of the surface air over the entire mid–high latitudes. The cold air and sea surface temperatures reached the lowest latitudes, strengthening the prevailing trades and shifting the ITCZ southward over all tropical ocean basins, away from the cold NH ice sheet/sea ice forcing (Fig. 11). The ITCZ prefers the warmer hemisphere, and as shown in Fig. 6, the southward shift of Hadley circulation also moves moisture from the NH to SH subtropics (Chiang and Bitz 2005; Broccoli et al. 2006; Chiang

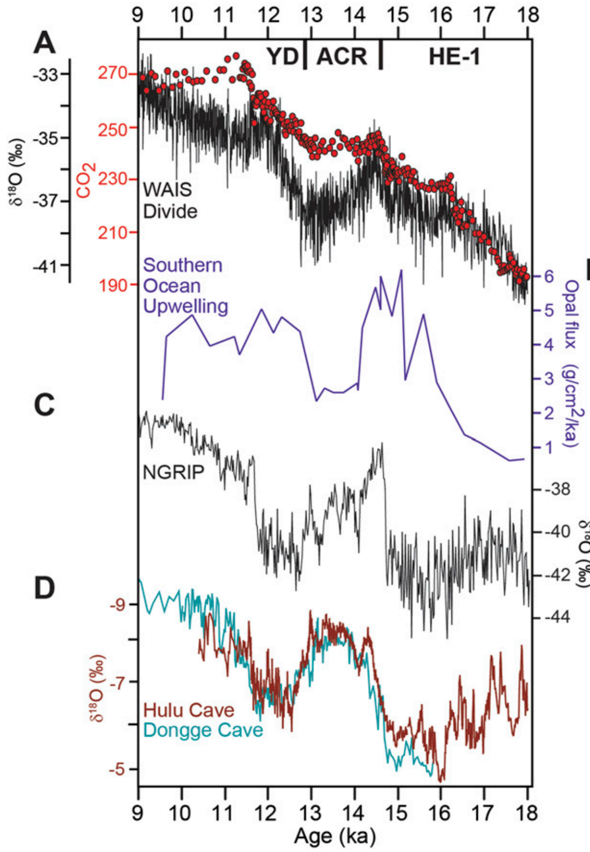

FIG. 12. Climate proxy records during the last glacial to interglacial transition: (a) $\delta^{18}O$ and CO_2 (ppmv) from West Antarctica (WAIS Divide Project Members 2013; Marcott et al. 2014); (b) Opal flux from sediment core TN057–13PC9 (Anderson et al. 2009); (c) $\delta^{18}O$ from the North Greenland Ice Core Project (Rasmussen et al. 2006) and (d) from the Hulu and Dongge Caves, China (Yuan et al. 2004). Also shown are timing of HE-1, Antarctic Cold Reversal (ACR), and YD following that used in references.

2009; Chiang and Friedman 2012). During the LGM, tropical climate must have been generally more arid than present because of colder temperatures (Seager et al. 2000); however, spatial variability of atmospheric moisture likely caused some areas to become wetter at times (Fig. 11c; Chiang and Friedman 2012).

During cold glacial periods, perhaps one of the most important hypothesized polar effects on the lower latitudes occurred during Heinrich events (Heinrich 1988). Heinrich events—defined as iceberg discharges into the North Atlantic (Heinrich 1988; Hemming 2004)—have been implicated in affecting oceanic deep water formation [Atlantic meridional overturning circulation (AMOC)], the westerlies in both hemispheres, and abrupt tropical and global climate changes (Anderson et al. 2009; Denton et al. 2010; Rhodes et al. 2015). The initiator or cause(s) of Heinrich events, which average a pacing of ~7000 years, remains unknown, but most ideas point to NH cooling and Laurentide Ice Sheet instability and collapse playing key roles (Hemming 2004). Several studies have built a hypothesis that links the North Atlantic high-latitude region to the tropics and ITCZ and to the SH middle–high latitudes during cold periods including Heinrich events (Fig. 12; Anderson et al. 2009; Timmermann et al. 2010; Toggweiler and Lea 2010; Denton et al. 2010). The idea is that at millennial time scales strong North Atlantic winter annual cooling, and expanded boreal winter/spring sea ice, may have affected the tropics, which in turn impacted the SH westerlies, Southern Ocean stratification, wind-driven upwelling, and CO_2 exchange with the atmosphere (Anderson et al. 2009; Denton et al. 2010; S.-Y. Lee et al. 2011). A southward shift of the westerly winds in the SH brings the core of the winds into latitudes where ocean ventilation and CO_2 exchange with the atmosphere occurs (Fig. 13). In addition, Chiang et al. (2014) hypothesized that a cool NH weakens monsoon intensity and the wintertime South Pacific subtropical jet, which in turn weakens the South Pacific split jet, leading to more zonally symmetric SH westerlies. A cold North Atlantic region in glacial periods hence causes a strong interhemispheric thermal gradient that connects the extratropics and tropics, and its effects reach even into the southern polar region (Chiang 2009; Chiang and Friedman 2012).

Specifically, the above hypothesis (i.e., Fig. 13) has been used to explain the chain of events (Fig. 12) from ~18 to 15 ka, during Heinrich Event 1 (HE-1), which led to SH middle–high latitude warming and the end of the last Ice Age or termination (Denton et al. 2010). During Heinrich Event 1, mean annual temperatures dropped by ~15°C around the North Atlantic sector, whereas in the SH middle latitudes, a rapid and pronounced summer warming of about 4°–5°C is documented from 18 to 15 ka (Putnam et al. 2013). A similar chain of events whereby cold winter North Atlantic temperatures are linked to a warm summer SH may have occurred during other millennial-scale climate events such as Younger Dryas (YD) stadial (Kaplan et al. 2010).

Modeling-based studies have focused on the hypothesized effect of a cold high-latitude glacial North Atlantic on the tropics and southern latitudes. For example, Timmermann et al. (2010) studied the tropical and global effects of a shutdown in AMOC. They observed that CO_2 changes that appear to accompany major disruptions of the AMOC can amplify Antarctic warming because of associated radiative forcing and polar amplification. S.-Y. Lee et al. (2011) examined the hypothesized effect of a cold glacial North Atlantic on the tropics, focusing on the Southern Hemisphere

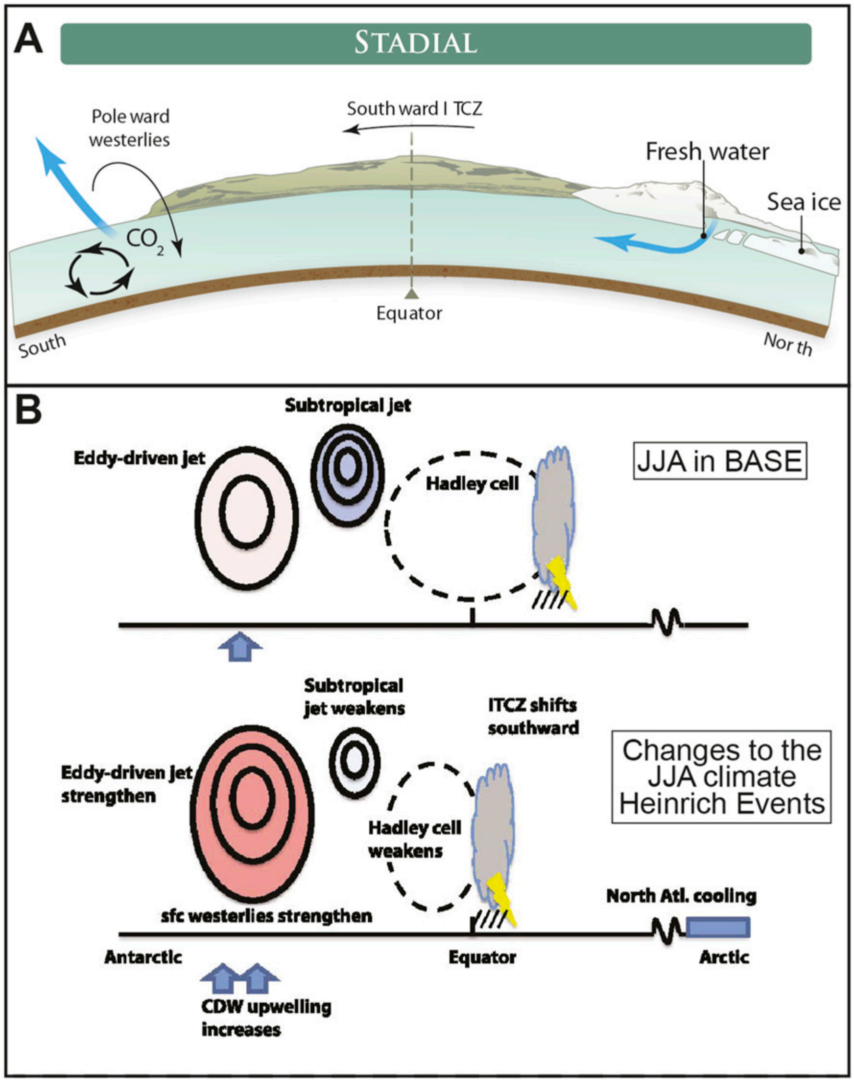

FIG. 13. How a polar–subpolar North Atlantic sector could have impacted the tropics during cold glacial and deglacial climates. The large NH ice sheets that exist during the Ice Age—and their attendant impacts on tropical climate—present scenarios for which we have no precise modern analogs (cf. Figs. 3 and 4). (a) From Anderson and Carr (2010), who reviewed a scenario whereby expanded winter sea ice in the North Atlantic, following a freshwater influx, induces a southward displacement or intensification of the southern westerlies. The change in winds causes increased exchange between surface and deep waters, releasing CO_2 into the atmosphere and helping to end an Ice Age (termination). The conceptual model is in part based on Anderson et al. (2009), Toggweiler and Lea (2010), and Denton et al. (2010). (b) S.-Y. Lee et al. (2011) examined the hypothesis presented in the top panel using the CCM, version 3.6. In (b), BASE represents the present climate; the bottom in (b) shows the hypothesized effects of extremely cold North Atlantic conditions, such as during Heinrich events (see text), including marked impacts to the ITCZ and Hadley cell, the effects of which can reach even the high southern latitudes and southern CDW, as envisioned in the top panel.

westerlies (Fig. 13b) during the last termination, using an atmospheric general circulation model [Community Climate Model (CCM3)]. They found that a North Atlantic cooling shifted the model intertropical convergence zone southward, weakening the southern branch of the Hadley circulation, and then the westerlies and wind stress over Southern Ocean increased by as much as 25%. S.-Y. Lee et al. (2011) further noted that such a cooling, mediated by tropical circulation shifting southward (Fig. 13), does not necessarily cause a simplistic shift of the low-latitude trade and Southern westerly wind belts, as proposed by the prior studies (cf. Chiang 2009; Anderson et al. 2009; Denton et al. 2010), but instead largely modulates the relative strengths of the subtropical and midlatitude eddy-driven jets and mid- and upper-tropospheric winds. They found one of the strongest effects is a strengthening of the westerlies over the South Pacific that is most pronounced in austral winter.

In general, models show no consistent response of the SH westerlies, nor a related atmospheric–oceanic CO_2 change to a shift in the winds, during the termination (e.g., Rojas 2013; Lauderdale et al. 2013; d'Orgeville et al. 2010). However, S.-Y. Lee et al. (2011) focused specifically on also simulating such shifts and the hypothesized (Anderson et al. 2009) biogeochemical effects (Fig. 13). They used the global monthly fields of wind stress from the CCM3 simulations described above in particular to force the Earth system model, the Minnesota Earth System Model for ocean biogeochemistry (MESMO), which incorporates interactive marine biogeochemistry (e.g., the biologic pump). When using CCMS output to force MESMO, they can simulate a glacial to interglacial CO_2 rise between 20 and 60 ppm. Although less than the glacial to interglacial change of ~100 ppm, a simulated increase of 20–60 ppm is a substantial fraction. Hence, S.-Y. Lee et al. (2011) concluded that an atmospheric teleconnection, mediated by tropical ITCZ response, could have played a critical role in bridging low- and high-latitude changes, and the CO_2 rise that helped usher in the end of the Ice Age (Figs. 12 and 13). However, S.-Y. Lee et al. (2011) did note the marine biologic response is still observationally unconstrained and unknown.

Regarding polar to tropical connections during cold glacial climates, we note three additional points. First, SH glacier and ice sheet changes were not as great as those in the north. Nonetheless, Southern Ocean ice expansion and a colder southern polar region in general would have increased polar amplification and its effects on low latitudes. For example, Marengo and Rogers (2001) discussed how mobile polar outbreaks would have been more common in both hemispheres, reaching the low tropical latitudes.

Second, recent hypotheses (discussed above) focus on a lead role for the atmosphere on lower-latitude climate changes during North Atlantic glacial cooling (e.g., Timmermann et al. 2010; Denton et al. 2010; Chiang et al. 2014; Fig. 13). Yet, these studies also point out that a key role for the atmosphere does not preclude prior ideas on the effect of ocean circulation in the phasing of interhemispheric climate events (e.g., Broecker 1998; Clement and Peterson 2008; Timmermann et al. 2010). A bipolar seesaw mechanism proposes curtailed North Atlantic meridional overturning circulation during abrupt climate changes and leads to heat being retained in the SH. Teasing apart the relative roles for oceanic and atmospheric pathways from paleorecords is difficult, although additional evidence from the tropics could at least implicate the importance of the latter atmospheric pathway (Anderson and Carr 2010).

Third, on glacial to interglacial time scales, one of the most important (but indirect) impacts the high latitudes may have on tropical climates is through changes in oceanic–atmospheric CO_2 exchange. For example, in the tropical Pacific, Ford et al. (2015) showed the zonal SST gradient was reduced and the thermocline on the eastern tropical Pacific was deeper during glacial times, and that these changes are consistent with a reduced CO_2 forcing. Ford et al. (2015) documented that during glacial times surface and subsurface temperatures in the western and eastern tropical Pacific were cooler by ~2.3°–2.4°C and 1.2°–1.3°C, respectively, compared with values in the late Holocene (Fig. 11). Sigman et al. (2010) argued the Southern Ocean CO_2 ''leak'' was reduced during Ice Ages. Oceanic CO_2 storage increased because of a colder circumpolar system and increased Southern Ocean stratification. Thus, high-latitude Southern Ocean processes may be responsible for one of the foremost internal feedbacks of glacial to interglacial cycles, with substantial consequences for tropical and global climates.

6. Summary and discussion

New advances in the recent decade in our understanding of the tropical–polar teleconnection come from several fronts. New studies have differentiated CP and EP El Niño events and their associated high-latitude responses. Studies also have identified different teleconnection characteristics associated with El Niño events and La Niña events. In addition, tropical to polar connections also have been identified at intraseasonal time scales associated with the MJO, and at decadal to multidecadal time scales as long-term trends in instrumental records. The known source areas that provide the tropical forcing to extratropics have expanded from the tropical Pacific to the North Atlantic, tropical Atlantic, and tropical Indian Ocean, as well as the subtropical South Pacific.

Rossby wave trains emanating from the tropics are still the main mechanism to explain the tropical and polar teleconnections from intraseasonal to multidecadal time scales. MJO emanates Rossby waves that propagate anomaly signals from the tropics to polar regions in a couple of weeks. Through this mechanism, the long-term changes in MJO phases can result in temperature and sea ice changes in polar regions of both hemispheres. Such changes contribute to 10%–20% polar warming in the Arctic. CP El Niño events generate a westward shift of the Rossby wave propagation compared to that excited by EP El Niño. Long-term SST trends in the central tropical Pacific and the tropical and North Atlantic are linked to the warming trends in the AP and West Antarctica through a variety of Rossby wave propagations. The Rossby wave propagation also exhibits strong seasonality, with a maximum wave propagation during austral spring in the SH. The upward propagating Rossby wave can disturb the stratosphere and associated anomaly signals then propagate down to the troposphere, impacting remote surface climate in 1–2 months. The stratosphere pathway is only effective with an active stratosphere (when SSWs occur).

Another mechanism that links a tropical forcing to high latitudes is altering the zonal wind system and mean meridional circulation. The warm SST in the tropics, particularly in the central tropical Pacific, impacts the subtropical jet through thermal wind balance and impacts the westerlies through eddy–mean flow interaction, consequently altering the mean meridional circulation. This zonally symmetric response is not affected by hemispheric seasonality and can directly influence the high-latitude climate modes NAM and SAM. These zonally symmetric responses in the zonal wind system operate at intraseasonal to multidecadal time scales. On the other hand, studies also have showed the regional meridional circulation has asymmetric responses to ENSO in the South Pacific and South Atlantic, which is associated with the SST contrast in the tropical Pacific and tropical Atlantic. This zonally asymmetric regional meridional circulation contributes to the ENSO–ADP connection.

Research over the last decade or so has also led to inferences that high-latitude modes interfere with tropical influences and produce either inconsistent ENSO impacts or long-term changes in the polar surface climate. SH high-latitude climate modes (SAM, wave 3, etc.) can either constructively or destructively interact with anomalous signals propagated from the tropics, resulting in a stronger or weaker teleconnection. Furthermore, the mean state of SAM has become more positive since the early 1990s, which has resulted in more ENSO–SAM in-phase variability (stronger tropical influences) compared with that in the 1980s. This change in the ENSO–SAM phase relationship has caused the long-term sea ice decline in the southeast Pacific and warming in the AP and West Antarctica.

In the past, tropical–polar teleconnections involved temperature gradients and thus a polar amplification different from present day. Possible past communications include those that exist at present, such as those mediated by Rossby wave trains and mean meridional circulation changes associated with ENSO (Fig. 3). Changes in orbital configuration and solar irradiance likely forced past tropical changes and consequently polar changes.

During Ice Age climates, a larger-than-present-day cryosphere existed over high latitudes, including ice sheets around the North Atlantic sector and expanded sea ice in the Southern Ocean. Cooling in the North Atlantic, for example, during Heinrich events, is hypothesized to have impacted the tropics and ITCZ through atmospheric teleconnections. The high-latitude influence may include Hadley circulation changes and modulation of the subtropical jets, and may have extended south of the equator well into SH latitudes. In the past, though, the poles and tropics may have had their greatest effects on each other simply by the fact that they play key roles in modulating global greenhouse gasses such as CO_2 (high southern latitudes), methane, and water vapor (e.g., tropics).

Despite great advances in describing and understanding the tropic–pole connections in the recent decade, unresolved scientific questions remain:

1) The connection between the MJO and southern high latitudes still remains poorly understood. Broadly, significant gaps exist in our knowledge of tropical–polar connections associated with the MJO and its interaction with high-latitude climate modes, and how and why the polar surface climate responds differently in the NH and SH winters to the long-term change of MJO.
2) How important is the role of tropical forcing in the polar amplification of global warming in winter? How do atmospheric heat and moisture transports (S. Lee et al. 2011; Yoo et al. 2012a) compare to other factors such as sea ice albedo–ocean memory (Screen and Simmonds 2010) and local heat turbulence fluxes due to the continuous decline of sea ice in the Barents and Kara Seas (Yang et al. 2016)?
3) Because of the complexity in the polar climate system due to the presence of sea ice and glacial meltwater export, climate models have large errors and uncertainties in polar regions, as revealed by the large model spread of climatological zonal-mean sea level pressure (Fig. 14). Recent studies (Turner et al. 2013; Shu et al. 2015) showed that simulated long-term trends of Antarctic sea ice in CMIP5 models are mostly opposite of the observations. On the other hand, some studies suggested that the observed

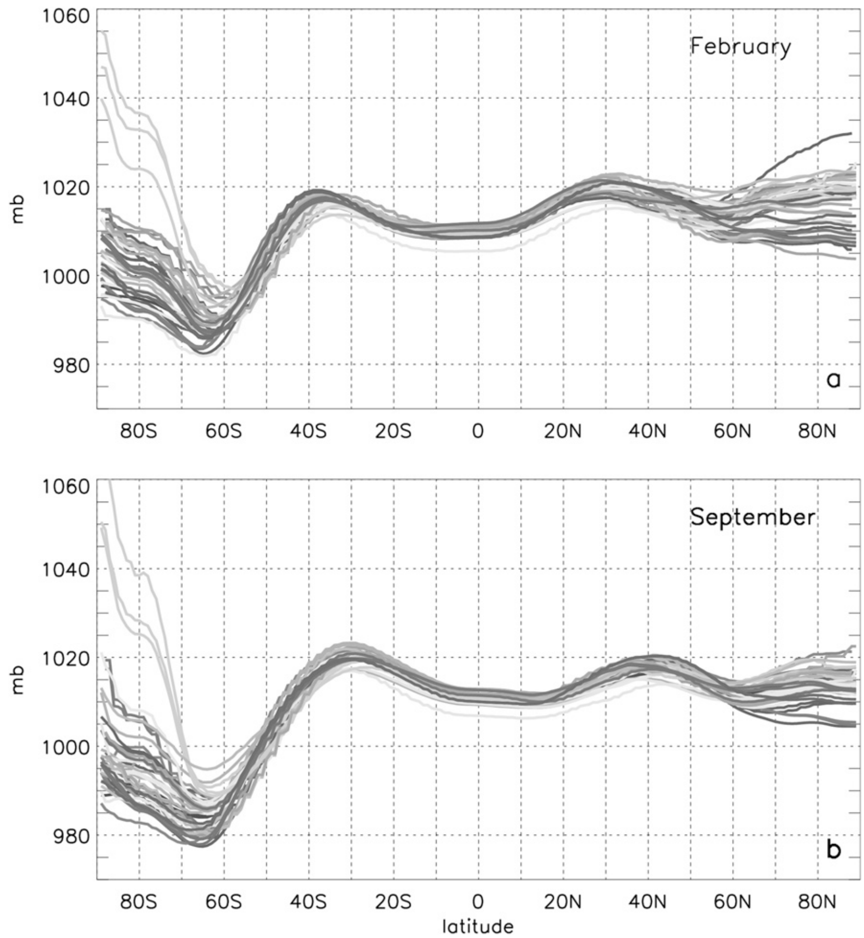

FIG. 14. Climatological zonal-mean sea level pressure for the period of 1901–2000 in (a) February and (b) September, derived from the historical run of 42 CIMP5 fully coupled climate models. The amplification of model uncertainties in the polar regions, particularly in the Antarctic, indicates the models' deficiencies in representing the atmosphere–ocean–sea ice coupled system as well as in representing the extreme environment of continental Antarctica.

trends in the total Antarctic extent are within the range of internal variability presented in these climate models (e.g., Bitz and Polvani 2012; Turner et al. 2013; Mahlstein et al. 2013; Polvani and Smith 2013; Swart and Fyfe 2013). However, Zunz et al. (2013) claim that CMIP5 models significantly overestimate natural variability after the long-term trends are removed. Likewise, Simmonds (2015) suggested that when the Antarctic sea ice extent experiences an accelerated increase during the last 35 years, the simulated natural variability decreases. Both studies question CMIP5 models' ability to test the hypothesis that the observed trends are within the range of internal variability that occurs in nature. Moreover, the dynamical processes in the atmosphere–ocean–sea ice system are quite different in the Arctic from those in the Antarctic. It is important for us to understand how well the dynamical processes are represented in CMIP5 models before we can utilize these models to understand the tropical–polar connection, and understand the paradoxical responses of polar regions to climate change. More direct communications among climate modelers, polar oceanographers, and climate scientists would greatly foster understanding on what CMIP5 models can offer and what the limitations are in these models in terms of investigating the tropical–polar connections.

4) New paleo datasets, especially in the SH where there are spatial and temporal gaps in data, are needed to understand the connections between polar cooling in both hemispheres and tropical effects, including the theoretical mechanisms (Chiang and Friedman 2012). Paleoclimate studies have stalwartly focused on polar effects on the tropics during Ice Ages (Fig. 13). Yet, low-latitude influences on high-latitude regions

must still occur during cold glacial periods, as well as during the warm interglacials such as present day. For example, paleostudies need to better understand the spatial–temporal pattern of ENSO, its effects at higher latitudes, and linkage and transition to dominant higher-latitude modes of variability such as SAM (Fig. 3). This includes reconstructions of past individual El Niño–La Niña events, as well as low-frequency changes. Signals of ENSO and other tropical forcings can be detected in polar proxy records such as ice cores; however, what is the magnitude of the effect relative to other high-latitude climate forcings?

In the last 10 years, great strides have been made in modeling paleoclimates, especially to understand the role of internal feedbacks and to capture broad paleoclimate patterns (e.g., Cane et al. 2006; Braconnot et al. 2012; Harrison et al. 2015). On the other hand, model experiments do not yet show consistent changes (or at least their magnitude), including those for past patterns of atmospheric and sea surface temperatures, such as for the SH westerlies (Rojas 2013) during the LGM and subsequent warming of the termination (e.g., Chavaillaz et al. 2013; Rojas et al. 2009; Rojas 2013). Models are also not consistent in terms of connections between the high-latitude glacial-age North Atlantic and the ITCZ (Kageyama et al. 2013), nor do most models show a pronounced CO_2 response to the positon of the southern westerlies, for example, as a result of high-latitude processes (e.g., Lauderdale et al. 2013; d'Orgeville et al. 2010).

5) Paleoclimatologists typically have to think about tropical–polar connections and processes that occur for the most part on decadal or longer time scales, due to dating resolution and proxy type. Exceptions exist for ice cores, but these are more or less limited to the polar regions and are of short duration in tropical sites. Also, tree ring–based efforts often only go back less than a millennium. On the other hand, paleorecords can provide a window into longer-term low-frequency changes and tropical–polar connections not evident or obvious in the short instrumental record. Better communication and integration of intellectual pursuits, especially between modernists and paleoscience communities, would reduce the limitations (e.g., different time scales) of the respective efforts, and help lead to resolution of key problems concerning tropical–polar connections (Yuan et al. 2015).

Acknowledgments. The authors gratefully acknowledge the Climate Center of Lamont-Doherty Earth Observatory and NASA GISS, and LDEO Director's Office for their generous support of the mini-conference "Connecting the Tropics to Polar Regions," which motivated the authors to write this paper. Yuan is supported by NSF Grant PLR-1443444 and Kaplan acknowledges NSF EAR-0902363. This is LDEO contribution number 8197.

REFERENCES

Anderson, R. F., and M.-E. Carr, 2010: Uncorking the Southern Ocean's vintage CO_2. *Science*, **328**, 1117–1118, https://doi.org/10.1126/science.1190765.

——, S. Ali, L. I. Bradtmiller, S. H. H. Nielsen, M. Q. Fleisher, B. E. Anderson, and L. H. Burckle, 2009: Wind-driven upwelling in the Southern Ocean and the deglacial rise in atmospheric CO_2. *Science*, **323**, 1443–1448, https://doi.org/10.1126/science.1167441.

Bals-Elsholz, T. M., E. H. Atallah, L. F. Bosart, T. A. Wasula, M. J. Cempa, and A. R. Lupo, 2001: The winter Southern Hemisphere split jet: Structure, variability, and evolution. *J. Climate*, **14**, 4191–4215, https://doi.org/10.1175/1520-0442(2001)014<4191:TWSHSJ>2.0.CO;2.

Barron, J. A., and L. Anderson, 2011: Enhanced late Holocene ENSO/PDO expression along the margins of the eastern North Pacific. *Quat. Int.*, **235**, 3–12, https://doi.org/10.1016/j.quaint.2010.02.026.

Bell, C. J., L. J. Gray, A. J. Charlton-Perez, M. M. Joshi, and A. A. Scaife, 2009: Stratospheric communication of El Niño teleconnections to European winter. *J. Climate*, **22**, 4083–4096, https://doi.org/10.1175/2009JCLI2717.1.

Bitz, C. M., and L. M. Polvani, 2012: Antarctic climate response to stratospheric ozone depletion in a fine resolution ocean climate model. *Geophys. Res. Lett.*, **39**, L20705, https://doi.org/10.1029/2012GL053393.

Braconnot, P., S. P. Harrison, M. Kageyama, P. J. Bartlein, V. Masson-Delmotte, A. Abe-Ouchi, B. Otto-Bliesner, and Y. Zhao, 2012: Evaluation of climate models using palaeoclimatic data. *Nat. Climate Change*, **2**, 417–424, https://doi.org/10.1038/nclimate1456.

Broccoli, A. J., K. A. Dahl, and R. J. Stouffer, 2006: Response of the ITCZ to Northern Hemisphere cooling. *Geosphys. Res. Lett.*, **33**, L01702, https://doi.org/10.1029/2005GL024546.

Broecker, W. S., 1998: Paleocean circulation during the last deglaciation: A bipolar seesaw? *Paleoceanography*, **13**, 119–121, https://doi.org/10.1029/97PA03707.

Bromwich, D. H., A. N. Rogers, P. Kållberg, R. I. Cullather, J. W. C. White, and K. J. Kreutz, 2000: ECMWF analyses and reanalyses depiction of ENSO signal in Antarctic precipitation. *J. Climate*, **13**, 1406–1420, https://doi.org/10.1175/1520-0442(2000)013<1406:EAARDO>2.0.CO;2.

——, J. P. Nicolas, A. J. Monaghan, M. A. Lazzara, L. M. Keller, G. A. Weidner, and A. B. Wilson, 2013: Central West Antarctica among the most rapidly warming regions on Earth. *Nat. Geosci.*, **6**, 139–145, https://doi.org/10.1038/ngeo1671.

Buizert, C., and Coauthors, 2015: The WAIS divide deep ice core WD2014 chronology—Part 1: Methane synchronization (68–31 ka BP) and the Gas Age–Ice Age difference. *Climate Past*, **11**, 153–173, https://doi.org/10.5194/cp-11-153-2015.

Butler, A. H., and L. M. Polvani, 2011: El Niño, La Niña, and stratospheric sudden warmings: A reevaluation in light of the observational record. *Geophys. Res. Lett.*, **38**, L13807, https://doi.org/10.1029/2011GL048084.

——, ——, and C. Deser, 2014: Separating the stratospheric and tropospheric pathways of El Niño–Southern Oscillation teleconnections. *Environ. Res. Lett.*, **9**, 024014, https://doi.org/10.1088/1748-9326/9/2/024014.

Cai, W., A. Sullivan, and T. Cowan, 2011: Interactions of ENSO, the IOD, and the SAM in CMIP3 models. *J. Climate*, **24**, 1688–1704, https://doi.org/10.1175/2010JCLI3744.1.

Cane, M. A., and Coauthors, 2006: Progress in paleoclimate modeling. *J. Climate*, **19**, 5031–5057, https://doi.org/10.1175/JCLI3899.1.

Carleton, A. M., and D. Whalley, 1988: Eddy transport of sensible heat and the life history of synoptic systems: A statistical analysis for the Southern Hemisphere winter. *Meteor. Atmos. Phys.*, **38**, 140–152, https://doi.org/10.1007/BF01029778.

——, and D. A. Carpenter, 1990: Satellite climatology of 'polar lows' and broadscale climatic associations for the Southern Hemisphere. *Int. J. Climatol.*, **10**, 219–246, https://doi.org/10.1002/joc.3370100302.

——, and M. Fitch, 1993: Synoptic aspects of Antarctic mesocyclones. *J. Geophys. Res.*, **98**, 12 997–13 018, https://doi.org/10.1029/92JD02132.

——, and Y. Song, 2000: Satellite passive sensing of the marine atmosphere associated with cold air mesoscale cyclones. *Prof. Geogr.*, **52**, 289–306, https://doi.org/10.1111/0033-0124.00225.

Carré, M., J. P. Sachs, S. Purca, A. J. Schauer, P. Braconnot, R. Angeles Falcón, M. Julien, and D. Lavallée, 2014: Holocene history of ENSO variance and asymmetry in the eastern tropical Pacific. *Science*, **345**, 1045–1048, https://doi.org/10.1126/science.1252220.

Cassou, C., 2008: Intraseasonal interaction between the Madden–Julian oscillation and the North Atlantic Oscillation. *Nature*, **455**, 523–527, https://doi.org/10.1038/nature07286.

——, and L. Terray, 2001: Ocean forcing of the wintertime low-frequency atmospheric variability in the North Atlantic European sector: A study with the ARPEGE model. *J. Climate*, **14**, 4266–4291, https://doi.org/10.1175/1520-0442(2001)014<4266:OFOTWL>2.0.CO;2.

Cavalieri, D. J., and C. L. Parkinson, 2012:Arctic sea ice variability and trends, 1979–2010. *Cryosphere*, **6**, 881–889, https://doi.org/10.5194/tc-6-881-2012.

Chapman, W. L., and J. E. Walsh, 2007: A synthesis of Antarctic temperatures. *J. Climate*, **20**, 4096–4117, https://doi.org/10.1175/JCLI4236.1.

Chavaillaz, Y., F. Codron, and M. Kageyama, 2013: Southern westerlies in LGM and future (RCP4.5) climates. *Climate Past*, **9**, 517–524, https://doi.org/10.5194/cp-9-517-2013.

Chen, B., S. R. Smith, and D. H. Bromwich, 1996: Evolution of the tropospheric split jet over the South Pacific Ocean during the 1986–89 ENSO cycle. *Mon. Wea. Rev.*, **124**, 1711–1731, https://doi.org/10.1175/1520-0493(1996)124<1711:EOTTSJ>2.0.CO;2.

Chiang, J. C. H., 2009: The tropics in paleoclimate. *Annu. Rev. Earth Planet. Sci.*, **37**, 263–297, https://doi.org/10.1146/annurev.earth.031208.100217.

——, and C. M. Bitz, 2005: Influence of high latitude ice cover on the marine Intertropical Convergence Zone. *Climate Dyn.*, **25**, 477–496, https://doi.org/10.1007/s00382-005-0040-5.

——, and A. R. Friedman, 2012: Extratropical cooling, interhemispheric thermal gradients, and tropical climate change. *Annu. Rev. Earth Planet. Sci.*, **40**, 383–412, https://doi.org/10.1146/annurev-earth-042711-105545.

——, S.-Y. Lee, A. E. Putnam, and X. Wang, 2014: South Pacific split jet, ITCZ shifts, and atmospheric north–south linkages during abrupt climate changes of the last glacial period. *Earth Planet. Sci. Lett.*, **406**, 233–246, https://doi.org/10.1016/j.epsl.2014.09.012.

Choi, J., S.-I. An, B. Dewitte, and W. W. Hsieh, 2009: Interactive feedback between the tropical Pacific decadal oscillation and ENSO in a coupled general circulation model. *J. Climate*, **22**, 6597–6611, https://doi.org/10.1175/2009JCLI2782.1.

Ciasto, L. M., G. R. Simpkins, and M. H. England, 2015: Teleconnections between tropical Pacific SST anomalies and extratropical Southern Hemisphere climate. *J. Climate*, **28**, 56–65, https://doi.org/10.1175/JCLI-D-14-00438.1.

Clegg, B. F., R. Kelly, G. H. Clarke, I. R. Walker, and F.-S. Hu, 2011: Nonlinear response of summer temperature to Holocene insolation forcing in Alaska. *Proc. Natl. Acad. Sci. USA*, **108**, 19 299–19 304, https://doi.org/10.1073/pnas.1110913108.

Clem, K. R., and R. L. Fogt, 2013: Varying roles of ENSO and SAM on the Antarctic Peninsula climate in austral spring. *J. Geophys. Res. Atmos.*, **118**, 11 481–11 492, https://doi.org/10.1002/jgrd.50860.

——, and ——, 2015: South Pacific circulation changes and their connection to the tropics and regional Antarctic warming in austral spring, 1979–2012. *J. Geophys. Res. Atmos.*, **120**, 2773–2792, https://doi.org/10.1002/2014JD022940.

——, and J. A. Renwick, 2015: Austral spring Southern Hemisphere circulation and temperature changes and links to the SPCZ. *J. Climate*, **28**, 7371–7384, https://doi.org/10.1175/JCLI-D-15-0125.1.

Clement, A. C., and L. C. Peterson, 2008: Mechanisms of abrupt climate change of the last glacial period. *Rev. Geophys.*, **46**, RG4002, https://doi.org/10.1029/2006RG000204.

——, R. Seager, and M. A. Cane, 2000: Suppression of El Niño during the mid-Holocene by changes in the earth's orbit. *Paleoceanography*, **15**, 731–737, https://doi.org/10.1029/1999PA000466.

Cobb, K. M., N. Westphal, H. R. Sayani, J. T. Watson, E. Di Lorenzo, H. Cheng, R. L. Edwards, and C. D. Charles, 2013: Highly variable El Niño–Southern Oscillation throughout the Holocene. *Science*, **339**, 67–70, https://doi.org/10.1126/science.1228246.

Cullather, R. I., D. H. Bromwich, and M. L. Van Woert, 1996: Interannual variations in Antarctic precipitation related to El Niño–Southern Oscillation. *J. Geophys. Res.*, **101**, 19 109–19 118, https://doi.org/10.1029/96JD01769.

Denton, G. H., R. F. Anderson, J. R. Toggweiler, R. L. Edwards, J. M. Schaefer, and A. E. Putnam, 2010: The last glacial termination. *Science*, **328**, 1652–1656, https://doi.org/10.1126/science.1184119.

Dewitte, B., S.-W. Yeh, B.-K. Moon, C. Cibot, and L. Terray, 2007: Rectification of the ENSO variability by interdecadal changes in the equatorial background mean state in a CGCM simulation. *J. Climate*, **20**, 2002–2021, https://doi.org/10.1175/JCLI4110.1.

Ding, Q., and E. J. Steig, 2013: Temperature change on the Antarctic Peninsula linked to the tropical Pacific. *J. Climate*, **26**, 7570–7585, https://doi.org/10.1175/JCLI-D-12-00729.1.

——, ——, D. S. Battisti, and M. Küttel, 2011: Winter warming in West Antarctica caused by central tropical Pacific warming. *Nat. Geosci.*, **4**, 398–403, https://doi.org/10.1038/ngeo1129.

——, ——, ——, and J. M. Wallace, 2012: Influence of the tropics on the southern annular mode. *J. Climate*, **25**, 6330–6348, https://doi.org/10.1175/JCLI-D-11-00523.1.

——, J. M. Wallace, D. S. Battisti, E. J. Steig, A. J. E. Gallant, H.-J. Kim, and L. Geng, 2014: Tropical forcing of the recent rapid Arctic warming in northeastern Canada and Greenland. *Nature*, **509**, 209–212, https://doi.org/10.1038/nature13260.

d'Orgeville, M., W. P. Sijp, M. H. England, and K. J. Meissner, 2010: On the control of glacial-interglacial atmospheric CO_2 variations by the Southern Hemisphere westerlies. *Geophys. Res. Lett.*, **37**, L21703, https://doi.org/10.1029/2010GL045261.

Dutrieux, P., and Coauthors, 2014: Strong sensitivity of Pine Island ice-shelf melting to climatic variability. *Science*, **343**, 174–178, https://doi.org/10.1126/science.1244341.

Emile-Geay, J., M. Cane, R. Seager, A. Kaplan, and P. Almasi, 2007: El Niño as a mediator of the solar influence on climate. *Paleoceanography*, **22**, PA3210, https://doi.org/10.1029/2006PA001304.

Flatau, M., and Y.-J. Kim, 2013: Interaction between the MJO and polar circulations. *J. Climate*, **26**, 3562–3574, https://doi.org/10.1175/JCLI-D-11-00508.1.

Fogt, R. L., and D. H. Bromwich, 2006: Decadal variability of the ENSO teleconnection to the high-latitude South Pacific governed by coupling with the southern annular mode. *J. Climate*, **19**, 979–997, https://doi.org/10.1175/JCLI3671.1.

——, ——, and K. M. Hines, 2011: Understanding the SAM influence on the South Pacific ENSO teleconnection. *Climate Dyn.*, **36**, 1555–1576, https://doi.org/10.1007/s00382-010-0905-0.

Ford, H. L., A. C. Ravelo, and P. J. Polissar, 2015: Reduced El Niño–Southern Oscillation during the Last Glacial Maximum. *Science*, **347**, 255–258, https://doi.org/10.1126/science.1258437.

Garfinkel, C. I., S. B. Feldstein, D. W. Waugh, C. Yoo, and S. Lee, 2012: Observed connection between stratospheric sudden warmings and the Madden–Julian oscillation. *Geophys. Res. Lett.*, **39**, L18807, https://doi.org/10.1029/2012GL053144.

Garreaud, R. D., and D. S. Battisti, 1999: Interannual (ENSO) and interdecadal (ENSO-like) variability in the Southern Hemisphere tropospheric circulation. *J. Climate*, **12**, 2113–2123, https://doi.org/10.1175/1520-0442(1999)012<2113:IEAIEL>2.0.CO;2.

Gloersen, P., 1995: Modulation of hemispheric sea-ice cover by ENSO events. *Nature*, **373**, 503–506, https://doi.org/10.1038/373503a0.

Graversen, R. G., 2006: Do changes in the midlatitude circulation have any impact on the Arctic surface air temperature trend? *J. Climate*, **19**, 5422–5438, https://doi.org/10.1175/JCLI3906.1.

Harangozo, S. A., 2000: A search for ENSO teleconnection teleconnections in the west Antarctic Peninsular climate in austral winter. *Int. J. Climatol.*, **20**, 663–678, https://doi.org/10.1002/(SICI)1097-0088(200005)20:6<663::AID-JOC493>3.0.CO;2-I.

Harrison, S. P., P. J. Bartlein, K. Izumi, G. Li, J. Annan, J. Hargreaves, P. Braconnot, and M. Kageyama, 2015: Evaluation of CMIP5 palaeo-simulations to improve climate projections. *Nat. Climate Change*, **5**, 735–743, https://doi.org/10.1038/nclimate2649.

Heinrich, H., 1988: Origin and consequences of cyclic ice rafting in the northeast Atlantic Ocean during the past 130,000 years. *Quat. Res.*, **29**, 142–152, https://doi.org/10.1016/0033-5894(88)90057-9.

Hemming, S. R.., 2004: Heinrich events: Massive late Pleistocene detritus layers of the North Atlantic and their global climate imprint. *Rev. Geophys.*, **42**, RG1005, https://doi.org/10.1029/2003RG000128.

Henderson, G. R., B. S. Barrett, and D. M. Lafleur, 2014: Arctic sea ice and the Madden–Julian oscillation (MJO). *Climate Dyn.*, **43**, 2185–2196, https://doi.org/10.1007/s00382-013-2043-y.

Hitchman, M. H., and M. J. Rogal, 2010: ENSO influences on Southern Hemisphere column ozone during the winter to spring transition. *J. Geophys. Res.*, **115**, D20104, https://doi.org/10.1029/2009JD012844.

Hurwitz, M. M., P. A. Newman, L. D. Oman, and A. M. Molod, 2011: Response of the Antarctic stratosphere to two types of El Niño events. *J. Atmos. Sci.*, **68**, 812–822, https://doi.org/10.1175/2011JAS3606.1.

——, C. I. Garfinkel, P. A. Newman, and L. D. Oman, 2013: Sensitivity of the atmospheric response to warm pool El Niño events to modeled SSTs and future climate forcings. *J. Geophys. Res. Atmos.*, **118**, 13 371–13 382, https://doi.org/10.1002/2013JD021051.

Ineson, S., and A. A. Scaife, 2009: The role of the stratosphere in the European climate response to El Niño. *Nat. Geosci.*, **2**, 32–36, https://doi.org/10.1038/ngeo381.

IPCC, 2013: *Climate Change 2013: The Physical Science Basis.* Cambridge University Press, 1535 pp., https://doi.org/10.1017/CBO9781107415324.

Jevrejeva, S., J. C. Moor, and A. Grinsted, 2003: Influence of the Arctic Oscillation and El Niño–Southern Oscillation (ENSO) on ice conditions in the Baltic sea: The wavelet approach. *J. Geophys. Res.*, **108**, 4677, https://doi.org/10.1029/2003JD003417.

Jin, D., and B. P. Kirtman, 2009: Why the Southern Hemisphere ENSO responses lead ENSO. *J. Geophys. Res.*, **114**, D23101, https://doi.org/10.1029/2009JD012657.

——, and ——, 2010: How the annual cycle affects the extratropical response to ENSO. *J. Geophys. Res.*, **115**, D06102, https://doi.org/10.1029/2009JD012660.

Kageyama, M., and Coauthors, 2013: Climatic impacts of fresh water hosing under Last Glacial Maximum conditions: A multi-model study. *Climate Past*, **9**, 935–953, https://doi.org/10.5194/cp-9-935-2013.

Kang, I.-S., H.-H. No, and F. Kucharski, 2015: ENSO amplitude modulation associated with the mean SST changes in the tropical central Pacific induced by Atlantic multidecadal oscillation. *J. Climate*, **27**, 7911–7920, https://doi.org/10.1175/JCLI-D-14-00018.1.

Kao, H.-Y., and J.-Y. Yu, 2009: Contrasting eastern Pacific and central Pacific types of El Niño. *J. Climate*, **22**, 615–632, https://doi.org/10.1175/2008JCLI2309.1.

Kaplan, M. R., and Coauthors, 2010: Glacier retreat in New Zealand during the Younger Dryas stadial. *Nature*, **467**, 194–197, https://doi.org/10.1038/nature09313.

——, and Coauthors, 2016: Patagonian and southern South Atlantic view of Holocene climate. *Quat. Sci. Rev.*, **141**, 112–125, https://doi.org/10.1016/j.quascirev.2016.03.014.

Karoly, D. J., 1989: Southern Hemisphere circulation features associated with El Niño–Southern Oscillation events. *J. Climate*, **2**, 1239–1252, https://doi.org/10.1175/1520-0442(1989)002<1239:SHCFAW>2.0.CO;2.

Kiladis, G. N., and K. C. Mo, 1998: Interannual and intraseasonal variability in the Southern Hemisphere. *Meteorology of the Southern Hemisphere*, *Meteor. Monogr.*, No. 49, Amer. Meteor. Soc., 307–337.

Koutavas, A., and S. Joanides, 2012: El Niño–Southern Oscillation extrema in the Holocene and Last Glacial Maximum. *Paleoceanography*, **27**, PA4208, https://doi.org/10.1029/2012PA002378.

Kreutz, K. J., P. A. Mayewski, I. I. Pittalwala, L. D. Meeker, M. S. Twickler, and S. I. Whitlow, 2000: Sea level pressure variability in the Amundsen Sea region inferred from West Antarctic glaciochemical record. *J. Geophys. Res.*, **105**, 4047–4059, https://doi.org/10.1029/1999JD901069.

Krishnamurti, T. N., S.-H. Chu, and W. Iglesias, 1986: On the sea level pressure of the Southern Oscillation. *Arch. Meteor. Geophys. Bioclimatol.*, **34A**, 385–425, https://doi.org/10.1007/BF02257768.

Kwok, R., and J. C. Comiso, 2002: Southern Ocean climate and sea ice anomalies associated with the Southern Oscillation. *J. Climate*, **15**, 487–501, https://doi.org/10.1175/1520-0442(2002)015<0487:SOCASI>2.0.CO;2.

Lauderdale, J. M., A. C. N. Garabato, K. I. C. Oliver, M. J. Follows, and R. G. Williams, 2013: Wind-driven changes in Southern Ocean residual circulation, ocean carbon reservoirs and atmospheric CO_2. *Climate Dyn.*, **41**, 2145–2164, https://doi.org/10.1007/s00382-012-1650-3.

Lee, S., 2012: Testing of the tropically excited Arctic warming mechanism (TEAM) with traditional El Niño and La Niña. *J. Climate*, **25**, 4015–4022, https://doi.org/10.1175/jcli-d-12-00055.1.

——, T. Gong, N. Johnson, S. B. Feldstein, and D. Pollard, 2011: On the possible link between tropical convection and the Northern Hemisphere Arctic surface air temperature change between 1958 and 2001. *J. Climate*, **24**, 4350–4367, https://doi.org/10.1175/2011JCLI4003.1.

Lee, S.-Y., J. C. H. Chiang, K. Matsumoto, and K. S. Tokos, 2011: Southern Ocean wind response to North Atlantic cooling and the rise in atmospheric CO_2: Modeling perspective and paleoceanographic implications. *Paleoceanography*, **26**, PA1214, https://doi.org/10.1029/2010PA002004.

——, ——, and P. Chang, 2015: Tropical Pacific response to continental ice sheet topography. *Climate Dyn.*, **44**, 2429–2446, https://doi.org/10.1007/s00382-014-2162-0.

L'Heureux, M. L., and D. W. J. Thompson, 2006: Observed relationship between the El Niño–Southern Oscillation and the extratropical zonal-mean circulation. *J. Climate*, **19**, 276–287, https://doi.org/10.1175/JCLI3617.1.

——, and R. W. Higgins, 2008: Boreal winter links between the Madden–Julian oscillation and the Arctic Oscillation. *J. Climate*, **21**, 3040–3050, https://doi.org/10.1175/2007JCLI1955.1.

Li, X., D. M. Holland, E. P. Gerber, and C. Yoo, 2014: Impacts of the North and tropical Atlantic Ocean on the Antarctic Peninsula and sea ice. *Nature*, **505**, 538–542, https://doi.org/10.1038/nature12945.

Liu, J., X. Yuan, D. Rind, and D. G. Martinson, 2002: Mechanism study of the ENSO and southern high latitude climate teleconnections. *Geophys. Res. Lett.*, **29**, 1679, https://doi.org/10.1029/2002GL015143.

——, J. A. Curry, and D. G. Martinson, 2004: Interpretation of recent Antarctic sea ice variability. *Geophys. Res. Lett.*, **31**, L02205, https://doi.org/10.1029/2003GL018732.

Loewe, P., and G. Koslowski, 1998: The western Baltic Sea ice season in terms of a mass-related severity index 1879–1992. *Tellus*, **50A**, 219–241, https://doi.org/10.1034/j.1600-0870.1998.t01-1-00005.x.

Mahlstein, I., P. R. Gent, and S. Solomon, 2013: Historical Antarctic mean sea ice area, sea ice trends, and winds in CMIP5 simulations. *J. Geophys. Res.*, **118**, 5105–5110, https://doi.org/10.1002/jgrd.50443.

Marcott, S. A., and Coauthors, 2014: Centennial-scale changes in the global carbon cycle during the last deglaciation. *Nature*, **514**, 616–619, https://doi.org/10.1038/nature13799.

Marengo, J. A., and J. C. Rogers, 2001: Polar air outbreaks in the Americas: Assessments and impacts during modern and past climates. *Interhemispheric Climate Linkages*, V. Markgraf, Ed., Academic Press, 31–51.

Marshall, G. J., J. Turner, and W. D. Miners, 1998: Interpreting recent accumulation records through an understanding of the regional synoptic climatology: An example from the southern Antarctic Peninsula. *Ann. Glaciol.*, **27**, 610–616, https://doi.org/10.3189/1998AoG27-1-610-616.

Martinson, D. G., and R. A. Iannuzzi, 2003: Spatial/temporal patterns in Weddell gyre characteristics and their relationship to global climate. *J. Geophys. Res.*, **108**, 8083, https://doi.org/10.1029/2000JC000538.

Matthews, A. J., and M. P. Meredith, 2004: Variability of Antarctic circumpolar transport and the southern annular mode associated with the Madden–Julian oscillation. *Geophys. Res. Lett.*, **31**, L24312, https://doi.org/10.1029/2004GL021666.

Mayewski, P. A., and Coauthors, 2009: State of the Antarctic and Southern Ocean climate system (SASOCS). *Rev. Geophys.*, **47**, RG1003, https://doi.org/10.1029/2007RG000231.

McKee, D. C., X. Yuan, A. L. Gordon, B. A. Huber, and Z. Dong, 2011: Climate impact on interannual variability of Weddell Sea Bottom Water. *J. Geophys. Res.*, **116**, C05020, https://doi.org/10.1029/2010JC006484.

Meehl, G. A., J. M. Arblaster, C. M. Bitz, C. T. Y. Chung, and H. Teng, 2016: Antarctic sea-ice expansion between 2000 and 2014 driven by tropical Pacific decadal climate variability. *Nat. Geosci.*, **9**, 590–595, https://doi.org/10.1038/ngeo2751.

Meyerson, E. A., P. A. Mayewski, K. J. Kreutz, L. D. Meeker, S. I. Whitlow, and M. S. Twickler, 2002: The polar expression of ENSO and sea-ice variability as recorded in a South Pole ice core. *Ann. Glaciol.*, **35**, 430–436, https://doi.org/10.3189/172756402781817149.

Mitchell, L., E. Brook, J. E. Lee, C. Buizert, and T. Sowers, 2013: Constraints on the late Holocene anthropogenic contribution to the atmospheric methane budget. *Science*, **342**, 964–966, https://doi.org/10.1126/science.1238920.

Mo, K. C., and G. H. White, 1985: Teleconnections in the Southern Hemisphere. *Mon. Wea. Rev.*, **113**, 22–37, https://doi.org/10.1175/1520-0493(1985)113<0022:TITSH>2.0.CO;2.

——, and R. W. Higgins, 1998: The Pacific–South America modes and tropical convection during the Southern Hemisphere winter. *Mon. Wea. Rev.*, **126**, 1581–1596, https://doi.org/10.1175/1520-0493(1998)126<1581:TPSAMA>2.0.CO;2.

Molnar, P., and M. A. Cane, 2007: Early Pliocene (pre-Ice Age) El Niño-like global climate: Which El Niño? *Geosphere*, **3**, 337–365, https://doi.org/10.1130/GES00103.1.

Moreno, P. I., and J. Videla, 2016: Centennial and millennial-scale hydroclimate changes in northwestern Patagonia since 16,000 yr BP. *Quat. Sci. Rev.*, **149**, 326–337, https://doi.org/10.1016/j.quascirev.2016.08.008.

——, I. Vilanova, R. Villa-Martínez, R. D. Garreaud, M. Rojas, and R. de Pol-Holz, 2014: Southern annular mode-like changes in southwestern Patagonia at centennial timescales over the last three millennia. *Nat. Commun.*, **5**, 4375, https://doi.org/10.1038/ncomms5375.

Moy, C. M., G. O. Seltzer, D. T. Rodbell, and D. M. Anderson, 2002: Variability of El Niño/Southern Oscillation activity at millennial timescales during the Holocene epoch. *Nature*, **420**, 162–165, https://doi.org/10.1038/nature01194.

——, P. I. Moreno, R. B. Dunbar, M. R. Kaplan, J.-P. Francois, R. Villalba, and T. Haberzettle, 2009: Climate change in southern South America during the last two millennia. *Past Climate Variability in South America and Surrounding Regions from the Last Glacial Maximum to the Holocene*, F. Vimeux et al., Eds., Developments in Paleoenvironmental Research Series, Vol. 14, Springer, 353–393.

Nicolas, J. P., and D. H. Bromwich, 2014: New reconstruction of Antarctic near-surface temperatures: Multidecadal trends and reliability of global reanalyses. *J. Climate*, **27**, 8070–8093, https://doi.org/10.1175/JCLI-D-13-00733.1.

Noone, D., J. Turner, and R. Mulvaney, 1999: Atmospheric signals and characteristics of accumulation in Dronning Maud Land, Antarctica. *J. Geophys. Res.*, **104**, 19 191–19 211, https://doi.org/10.1029/1999JD900376.

Nuncio, M., and X. Yuan, 2015: The influence of the Indian Ocean dipole on Antarctic sea ice. *J. Climate*, **28**, 2682–2690, https://doi.org/10.1175/JCLI-D-14-00390.1.

——, A. J. Luis, and X. Yuan, 2011: Topographic meandering of Antarctic Circumpolar Current and Antarctic circumpolar wave in the ice-ocean-atmosphere system. *Geophys. Res. Lett.*, **38**, L13708, https://doi.org/10.1029/2011GL046898.

O'Donnell, R., N. Lewis, S. McIntyre, and J. Condon, 2011: Improved methods for PCA-based reconstructions: Case study using the Steig et al. (2009) Antarctic temperature reconstruction. *J. Climate* **24**, 2099–2115, https://doi.org/10.1175/2010JCLI3656.1.

Okumura, Y. M., D. Schneider, C. Deser, and R. Wilson, 2012: Decadal–interdecadal climate variability over Antarctica and linkages to the tropics: Analysis of ice core, instrumental, and tropical proxy data. *J. Climate*, **25**, 7421–7441, https://doi.org/10.1175/JCLI-D-12-00050.1.

Ortiz Beviá, M. J., I. Pérez-González, F. J. Alvarez-García, and A. Gershunov, 2010: Nonlinear estimation of El Niño impact on the North Atlantic winter. *J. Geophys. Res.*, **115**, D21123, https://doi.org/10.1029/2009JD013387.

PALAEOSENS Project Members, 2012: Making sense of palaeoclimate sensitivity. *Nature*, **491**, 683–691, https://doi.org/10.1038/nature11574.

Pohl, B., N. Fauchereau, C. J. C. Reason, and M. Rouault, 2010: Relationships between the Antarctic Oscillation, the Madden–Julian oscillation, and ENSO, and consequences for rainfall analysis. *J. Climate*, **23**, 238–254, https://doi.org/10.1175/2009JCLI2443.1.

Polvani, L. M., and K. L. Smith, 2013: Can natural variability explain observed Antarctic sea ice trends? New modeling evidence from CMIP5. *Geophy. Res. Lett.*, **40**, 3195–3199, https://doi.org/10.1002/grl.50578.

Pozo-Vázquez, D., S. R. Gámiz-Fortis, J. Tovar-Pescador, M. J. Esteban-Parra, and Y. Castro-Díez, 2005: North Atlantic winter SLP anomalies based on the autumn ENSO state. *J. Climate*, **18**, 97–130, https://doi.org/10.1175/JCLI-3210.1.

Previdi, M., and L. M. Polvani, 2014: Climate system response to stratospheric ozone depletion and recovery. *Quart. J. Roy. Meteor. Soc.*, **140**, 2401–2419, https://doi.org/10.1002/qj.2330.

Putnam, A. E., and Coauthors, 2013: Warming and glacier recession in the Rakaia Valley, Southern Alps of New Zealand, during Heinrich stadial 1. *Earth Planet. Sci. Lett.*, **382**, 98–110, https://doi.org/10.1016/j.epsl.2013.09.005.

Raphael, M. N., 2004: A zonal wave 3 index for the Southern Hemisphere. *Geophys. Res. Lett.*, **31**, L23212, https://doi.org/10.1029/2004GL020365.

Rasmussen, S. O., and Coauthors, 2006: A new Greenland ice core chronology for the last glacial termination. *J. Geophys. Res.*, **111**, D06102, https://doi.org/10.1029/2005JD006079.

Renwick, J. A., 1998: ENSO-related variability in the frequency of South Pacific blocking. *Mon. Wea. Rev.*, **126**, 3117–3123, https://doi.org/10.1175/1520-0493(1998)126<3117:ERVITF>2.0.CO;2.

Rhodes, R. H., E. J. Brook, J. C. H. Chiang, T. Blunier, O. J. Maselli, J. R. McConnell, D. Romanini, and J. P. Severinghaus, 2015: Enhanced tropical methane production in response to iceberg discharge in the North Atlantic. *Science*, **348**, 1016–1019, https://doi.org/10.1126/science.1262005.

Robinson, W. A., 2002: On the midlatitude thermal response to tropical warmth. *Geophys. Res. Lett.*, **29**, 1190, https://doi.org/10.1029/2001GL014158.

Rodgers, K. B., P. Friederichs, and M. Latif, 2004: Tropical Pacific decadal variability and its relation to decadal modulations of ENSO. *J. Climate*, **17**, 3761–3774, https://doi.org/10.1175/1520-0442(2004)017<3761:TPDVAI>2.0.CO;2.

Rojas, M., 2013: Sensitivity of Southern Hemisphere circulation to LGM and 4 × CO2 climates. *Geophys. Res. Lett.*, **40**, 965–970, https://doi.org/10.1002/grl.50195.

——, and Coauthors, 2009: The southern westerlies during the last glacial maximum in PMIP2 simulations. *Climate Dyn.*, **32**, 525–548, https://doi.org/10.1007/s00382-008-0421-7.

Sakaeda, N., and P. E. Roundy, 2014: The role of interactions between multiscale circulations in the observed zonally averaged zonal wind variability associated with the Madden–Julian oscillation. *J. Atmos. Sci.*, **71**, 3816–3836, https://doi.org/10.1175/JAS-D-13-0304.1.

Schneider, D. P., Y. Okumura, and C. Deser, 2012a: Observed Antarctic interannual climate variability and tropical linkages. *J. Climate*, **25**, 4048–4066, https://doi.org/10.1175/JCLI-D-11-00273.1.

——, C. Deser, and Y. Okumura, 2012b: An assessment and interpretation of the observed warming of West Antarctica in the austral spring. *Climate Dyn.*, **38**, 323–347, https://doi.org/10.1007/s00382-010-0985-x.

——, ——, and T. Fan, 2015: Comparing the impacts of tropical SST variability and polar stratospheric ozone loss on the Southern Ocean westerly winds. *J. Climate*, **28**, 9350–9372, https://doi.org/10.1175/JCLI-D-15-0090.1.

Screen, J. A., and I. Simmonds, 2010: The central role of diminishing sea ice in recent Arctic temperature amplification. *Nature*, **464**, 1334–1337, https://doi.org/10.1038/nature09051.

——, C. Deser, and I. Simmonds, 2012: Local and remote controls on observed Arctic warming. *Geophys. Res. Lett.*, **39**, L10709, https://doi.org/10.1029/2012GL051598.

Seager, R., A. C. Clement, and M. A. Cane, 2000: Glacial cooling in the tropics: Exploring the roles of tropospheric water vapor, surface wind speed, and boundary layer processes. *J. Atmos. Sci.*, **57**, 2144–2157, https://doi.org/10.1175/1520-0469(2000)057<2144:GCITTE>2.0.CO;2.

——, N. Harnik, Y. Kushnir, W. Robinson, and J. Miller, 2003: Mechanisms of hemispherically symmetric climate variability. *J. Climate*, **16**, 2960–2978, https://doi.org/10.1175/1520-0442(2003)016<2960:MOHSCV>2.0.CO;2.

Shao, Z.-D., and C.-Q. Ke, 2015: Spring–summer albedo variations of Antarctic sea ice from 1982 to 2009. *Environ. Res. Lett.*, **10**, 064001, https://doi.org/10.1088/1748-9326/10/6/064001.

Shu, Q., Z. Song, and F. Qiao, 2015: Assessment of sea ice simulations in the CMIP5 models. *Cryosphere*, **9**, 399–409, https://doi.org/10.5194/tc-9-399-2015.

Sigman, D. M., M. P. Hain, and G. H. Haug, 2010: The polar ocean and glacial cycles in atmospheric CO_2 concentration. *Nature*, **466**, 47–55, https://doi.org/10.1038/nature09149.

Simmonds, I., 2015: Comparing and contrasting the behaviour of Arctic and Antarctic sea ice over the 35 year period 1979–2013. *Ann. Glaciol.*, **56**, 18–28, https://doi.org/10.3189/2015AoG69A909.

——, and T. H. Jacka, 1995: Relationships between the interannual variability of Antarctic sea ice and the Southern Oscillation. *J. Climate*, **8**, 637–647, https://doi.org/10.1175/1520-0442(1995)008<0637:RBTIVO>2.0.CO;2.

Simpkins, G. R., S. McGregor, A. S. Taschetto, L. M. Ciasto, and M. H. England, 2014: Tropical connections to climatic change in the extratropical Southern Hemisphere: The role of Atlantic SST trends. *J. Climate*, **27**, 4923–4936, https://doi.org/10.1175/JCLI-D-13-00615.1.

Sinclair, M. R., J. A. Renwick, and J. W. Kidson, 1997: Low-frequency variability of Southern Hemisphere sea level pressure and weather system activity. *Mon. Wea. Rev.*, **125**, 2531–2543, https://doi.org/10.1175/1520-0493(1997)125<2531:LFVOSH>2.0.CO;2.

Sjögersten, S., C. R. Black, S. Evers, J. Hoyos-Santillan, E. L. Wright, and B. L. Turner, 2014: Tropical wetlands: A missing link in the global carbon cycle? *Global Biogeochem. Cycles*, **28**, 1371–1386, https://doi.org/10.1002/2014GB004844.

Smith, S. R., and C. R. Stearns, 1993: Antarctic pressure and temperature anomalies surrounding the minimum in the Southern Oscillation index. *J. Geophys. Res.*, **98**, 13 071–13 083, https://doi.org/10.1029/92JD02157.

Solomina, O. N, and Coauthors, 2015: Holocene glacier fluctuations. *Quat. Sci. Rev.*, **111**, 9–34, https://doi.org/10.1016/j.quascirev.2014.11.018.

Stammerjohn, S. E., D. G. Martinson, R. C. Smith, X. Yuan, and D. Rind, 2008: Trends in Antarctic annual sea ice retreat and advance and their relation to El Niño–Southern Oscillation and southern annular mode variability. *J. Geophys. Res.*, **113**, C03S90, https://doi.org/10.1029/2007JC004269.

Steig, E. J., Q. Ding, D. S. Battisti, and A. Jenkins, 2012: Tropical forcing of circumpolar deep water inflow and outlet glacier thinning in the Amundsen Sea embayment, West Antarctica. *Ann. Glaciol.*, **53**, 19–28, https://doi.org/10.3189/2012AoG60A110.

Sun, D., F. Xue, and T. Zhou, 2013: Impact of two types of El Niño on atmospheric circulation in the Southern Hemisphere. *Adv. Atmos. Sci.*, **30**, 1732–1742, https://doi.org/10.1007/s00376-013-2287-9.

Sun, F., and J.-Y. Yu, 2009: A 10–15-yr modulation cycle of ENSO intensity. *J. Climate*, **22**, 1718–1735, https://doi.org/10.1175/2008JCLI2285.1.

Swart, N. C., and J. C. Fyfe, 2013: The influence of recent Antarctic ice sheet retreat on simulated sea ice area trends. *Geophys. Res. Lett.*, **40**, 4328–4332, https://doi.org/10.1002/grl.50820.

Thompson, D. W. J., and S. Solomon, 2002: Interpretation of recent Southern Hemisphere climate change. *Science*, **296**, 895–899, https://doi.org/10.1126/science.1069270.

——, ——, P. J. Kushner, M. H. England, K. M. Grise, and D. J. Karoly, 2011: Signatures of the Antarctic ozone hole in Southern Hemisphere surface climate change. *Nat. Geosci.*, **4**, 741–749, https://doi.org/10.1038/ngeo1296.

Timmermann, A., 2003: Decadal ENSO amplitude modulations: A nonlinear paradigm. *Global Planet. Change*, **37**, 135–156, https://doi.org/10.1016/S0921-8181(02)00194-7.

——, and Coauthors, 2010: Towards a quantitative understanding of millennial-scale Antarctic warming events. *Quat. Sci. Rev.*, **29**, 74–85, https://doi.org/10.1016/j.quascirev.2009.06.021.

Toggweiler, J. R., and D. W. Lea, 2010: Temperature differences between the hemispheres and Ice Age climate variability. *Paleoceanography*, **25**, PA2212, https://doi.org/10.1029/2009PA001758.

Trenberth, K. E., and D. J. Shea, 1987: On the evolution of the Southern Oscillation. *Mon. Wea. Rev.*, **115**, 3078–3096, https://doi.org/10.1175/1520-0493(1987)115<3078:OTEOTS>2.0.CO;2.

——, G. W. Branstator, D. Karoly, A. Kumar, N.-C. Lau, and C. Ropelewski, 1998: Progress during TOGA in understanding and modeling global teleconnections associated with tropical sea surface temperatures. *J. Geophys. Res.*, **103**, 14 291–14 324, https://doi.org/10.1029/97JC01444.

Turner, J., 2004: The El Niño–Southern Oscillation and Antarctica. *Int. J. Climatol.*, **24**, 1–31, https://doi.org/10.1002/joc.965.

——, and Coauthors, 2009: Non-annular atmospheric circulation change induced by stratospheric ozone depletion and its role in the recent increase of Antarctic sea ice extent. *Geophys. Res. Lett.*, **36**, L08502, https://doi.org/10.1029/2009GL037524.

——, T. Phillips, J. S. Hosking, G. J. Marshall, and A. Orr, 2013: The Amundsen Sea low. *Int. J. Climatol.*, **33**, 1818–1829, https://doi.org/10.1002/joc.3558.

——, and Coauthors, 2016: Absence of 21st century warming on Antarctic Peninsula consistent with natural variability. *Nature*, **535**, 411–415, https://doi.org/10.1038/nature18645.

van Loon, H., and D. J. Shea, 1985: The Southern Oscillation. Part IV: The precursors south of 15°S to the extremes of the oscillation. *Mon. Wea. Rev.*, **113**, 2063–2074, https://doi.org/10.1175/1520-0493(1985)113<2063:TSOPIT>2.0.CO;2.

Venegas, S. A., and L. A. Mysak, 2000: Is there a dominant timescale of natural climate variability in the Arctic? *J. Climate*, **13**, 3412–3434, https://doi.org/10.1175/1520-0442(2000)013<3412:ITADTO>2.0.CO;2.

Villalba, R., 2007: Tree-ring evidence for tropical-extratropical influences on climate variability along the Andes in South America. *PAGES News*, Vol. 15, PAGES International Project Office, Bern, Switzerland, 23–25, https://doi.org/10.22498/pages.15.2.23.

——, E. R. Cook, R. D. D'Arrigo, G. C. Jacoby, P. D. Jones, M. J. Salinger, and J. Palmer, 1997: Sea-level pressure variability around Antarctica since A.D. 1750 inferred from subantarctic tree-ring records. *Climate Dyn.*, **13**, 375–390, https://doi.org/10.1007/s003820050172.

——, M. H. Masiokas, T. Kitzberger, and J. A. Boninsegna, 2005: Biogeographical consequences of recent climate changes in the southern Andes of Argentina. *Global Change and Mountain Regions*, U. M. Huber et al., Eds., Advances in Global Change Research, Vol. 23, Springer, 157–166.

——, and Coauthors, 2012: Unusual Southern Hemisphere tree growth patterns induced by changes in the southern annular mode. *Nat. Geosci.*, **5**, 793–798, https://doi.org/10.1038/ngeo1613.

WAIS Divide Project Members, 2013: Onset of deglacial warming in West Antarctic driven by local orbital forcing. *Nature*, **500**, 440–444, https://doi.org/10.1038/nature12376.

Webb, D. J., and B. A. de Cuevas, 2002: An ocean resonance in the southeast Pacific. *Geophys. Res. Lett.*, **29**, 1252, https://doi.org/10.1029/2001GL014259.

Wilson, A. B., D. H. Bromwich, K. M. Hines, and S.-H. Wang, 2014: El Niño flavors and their simulated impacts on atmospheric circulation in the high southern latitudes. *J. Climate*, **27**, 8934–8955, https://doi.org/10.1175/JCLI-D-14-00296.1.

——, ——, and ——, 2016: Simulating the mutual forcing of anomalous high southern latitude atmospheric circulation by El Niño flavors and the southern annular mode. *J. Climate*, **29**, 2291–2309, https://doi.org/10.1175/JCLI-D-15-0361.1.

Yang, X.-Y., X. Yuan, and M. Ting, 2016: Dynamical link between Barents–Kara sea ice and the Arctic Oscillation. *J. Climate*, **29**, 5013–5122, https://doi.org/10.1175/JCLI-D-15-0669.1.

Yoo, C., S. B. Feldstein, and S. Lee, 2011: The impact of the Madden-Julian oscillation trend on the Arctic amplification of surface air temperature during the 1979–2008 boreal winter. *Geophys. Res. Lett.*, **38**, L24804, https://doi.org/10.1029/2011GL049881.

——, S. Lee, and S. B. Feldstein, 2012a: Arctic response to an MJO-like tropical heating in an idealized GCM. *J. Atmos. Sci.*, **69**, 2379–2393, https://doi.org/10.1175/JAS-D-11-0261.1.

——, ——, and ——, 2012b: Mechanisms of extratropical surface air temperature change in response to the Madden–Julian oscillation. *J. Climate*, **25**, 5777–5790, https://doi.org/10.1175/JCLI-D-11-00566.1.

——, ——, and ——, 2012c: The impact of the Madden–Julian oscillation trend on the Antarctic warming during the 1979–2008 austral winter. *Atmos. Sci. Lett.*, **13**, 194–199, https://doi.org/10.1002/asl.379.

——, S. B. Feldstein, and S. Lee, 2013: The prominence of a tropical convective signal in the wintertime Arctic temperature. *Atmos. Sci. Lett.*, **15**, 7–12, https://doi.org/10.1002/asl2.455.

Yu, J.-Y., and H.-Y. Kao, 2007: Decadal changes of ENSO persistence barrier in SST and ocean heat content indices: 1958–2001. *J. Geophys. Res.*, **112**, D13106, https://doi.org/10.1029/2006JD007715.

——, H. Paek, E. S. Saltzman, and T. Lee, 2015: The early 1990s change in ENSO–PSA–SAM relationships and its impact on Southern Hemisphere climate. *J. Climate*, **28**, 9393–9408, https://doi.org/10.1175/JCLI-D-15-0335.1.

Yuan, D., and Coauthors, 2004: Timing, duration, and transitions of the last interglacial Asian monsoon. *Science*, **304**, 575–578, https://doi.org/10.1126/science.1091220.

Yuan, X., 2004: ENSO-related impacts on Antarctic sea ice: A synthesis of phenomenon and mechanisms. *Antarct. Sci.*, **16**, 415–425, https://doi.org/10.1017/S0954102004002238.

——, and D. G. Martinson, 2000: Antarctic sea ice extent variability and its global connectivity. *J. Climate*, **13**, 1697–1717, https://doi.org/10.1175/1520-0442(2000)013<1697:ASIEVA>2.0.CO;2.

——, and ——, 2001: The Antarctic dipole and its predictability. *Geophys. Res. Lett.*, **28**, 3609–3612, https://doi.org/10.1029/2001GL012969.

——, and C. Li, 2008: Climate modes in southern high latitudes and their impacts on Antarctic sea ice. *J. Geophys. Res.*, **113**, C06S91, https://doi.org/10.1029/2006JC004067.

——, M. A. Cane, and M. R. Kaplan, 2015: Connecting the tropics to polar regions. *Eos, Trans. Amer. Geophys. Union*, **96**, https://doi.org/10.1029/2015EO027953.

Zhou, S., and A. J. Miller, 2005: The interaction of the Madden–Julian oscillation and the Arctic Oscillation. *J. Climate*, **18**, 143–159, https://doi.org/10.1175/JCLI3251.1.

Zubiaurre, I., and N. Calvo, 2012: The El Niño–Southern Oscillation (ENSO) Modoki signal in the stratosphere. *J. Geophys. Res.*, **117**, D04104, https://doi.org/10.1029/2011JD016690.

Zunz, V., H. Goosse, and F. Massonnet, 2013: How does internal variability influence the ability of CMIP5 models to reproduce the recent trend in Southern Ocean sea ice extent? *Cryosphere*, **7**, 451–468, https://doi.org/10.5194/tc-7-451-2013.